Synchrotron Radiation and Materials Science Applications

X-Ray Diffraction for Materials Science Application

203 McLaughlin Hall
March 13, 2:10 to 3:30 pm

Simon Clark
Advanced Light Source, LBNL and UCB E&PS

BERKELEY LAB

Learning objectives

1. Understand the advantages of a synchrotron source of x-ray diffraction
2. Understand the differences between single crystal and powder diffraction
3. Understand the differences between monochromatic and polychromatic diffraction
4. Appreciate the use of these techniques in investigating material science problems

Presentation plan

1. Why use synchrotron radiation?
2. Single crystal diffraction
    1. Polychromatic
    2. Monochromatic
3. Powder diffraction
    1. Monochromatic
    2. Polychromatic

Acknowledgements

Nobumichi Tomura	Microdiffraction
Simon Teat	Single crystal diffraction
Lyn McClusker	Powder build up

Why use a synchrotron for diffraction?

- High Brightness
  - Highest resolution
  - Smallest samples
- Continuous spread of wavelengths
  - Laue diffraction
- High energy (short wavelength)
  - High penetration, in-situ studies
- High intensity
  - Time resolved studies

Presentation plan

1. Why use synchrotron radiation?
2. Single crystal diffraction
    1. Polychromatic
    2. Monochromatic
3. Powder diffraction
    1. Monochromatic
    2. Polychromatic

Laue or monochromatic?

$$\lambda = 2d \sin \theta$$

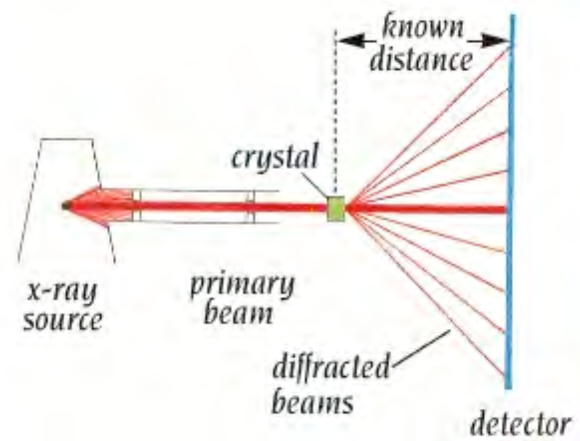

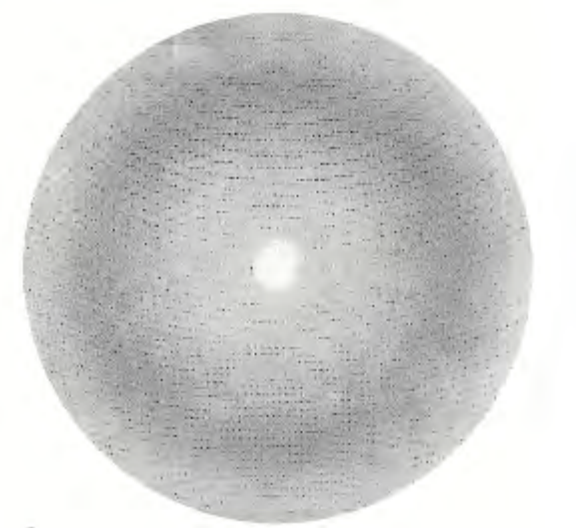

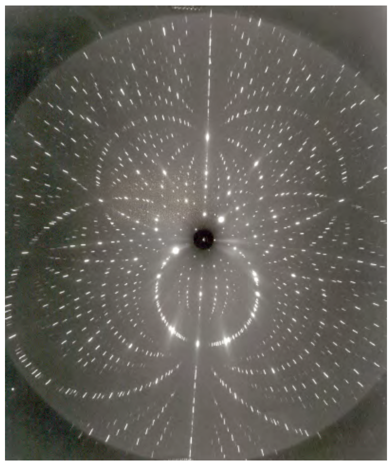

Pros and cons of Laue and Bragg?

Laue (polychromatic)

- One shot experiment
- Difficult to make intensity corrections
- Overload problem

Bragg (monochromatic)

- Takes many frames to get complete data set

Presentation plan

1. Why use synchrotron radiation?
2. Single crystal diffraction
    1. Polychromatic
    2. Monochromatic
3. Powder diffraction
    1. Monochromatic
    2. Polychromatic

Polychromatic (white) beam microdiffraction

Grain size > or ~ beam size

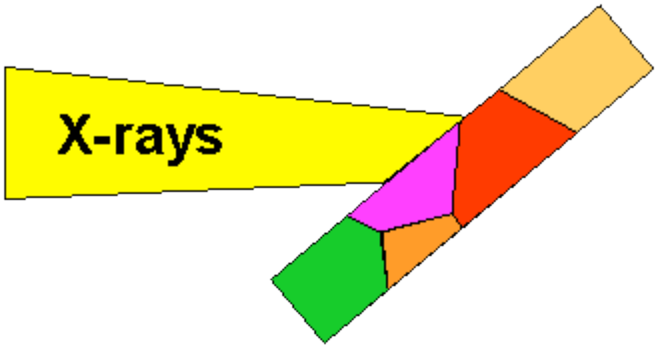

- Grain orientation mapping
- Crystalline phases distribution
- Strain/Stress mapping
- Local plasticity/dislocation densities

Monochromatic beam microdiffraction

Grain size << beam size

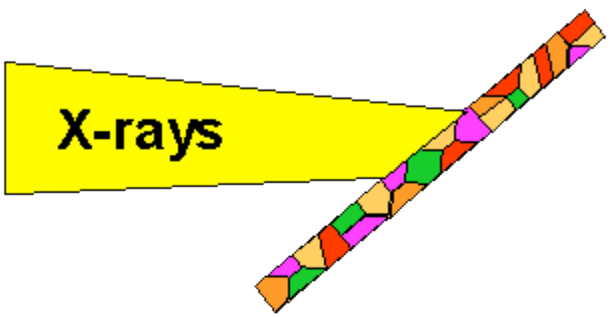

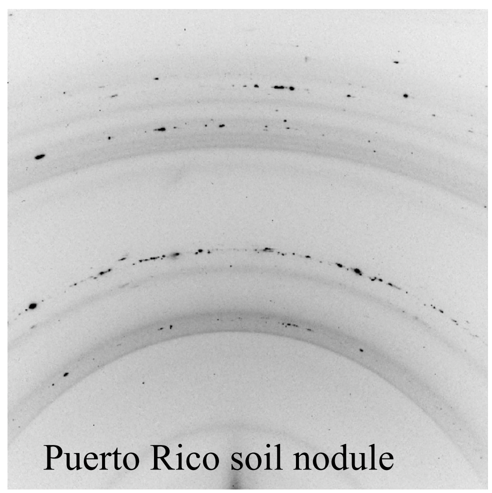

- Texture analysis
- Crystalline phases distribution
- Stress mapping

X-ray diffraction

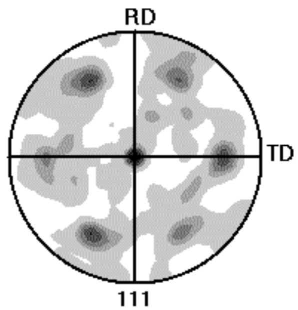

Pole figure of a Cu thin film on Si

Average texture and grain size

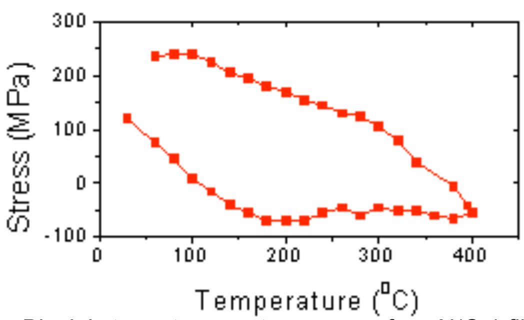

Biaxial stress-temperature curve of an Al(Cu) film on Si

Average strain/stress

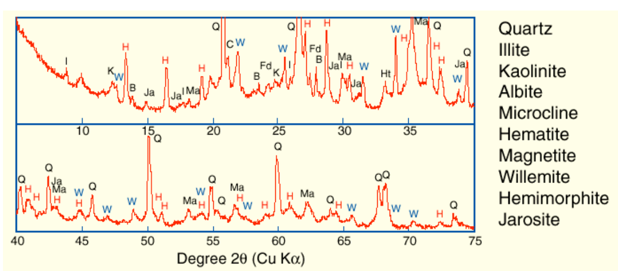

Average diffractogram of a ferromanganese soil nodule

Crystalline species identification

X-ray μ-diffraction

Grain map, grain orientation relationships, subgrains structure

Grain map of NiTi alloy

Local deformation and residual stress within individual grains

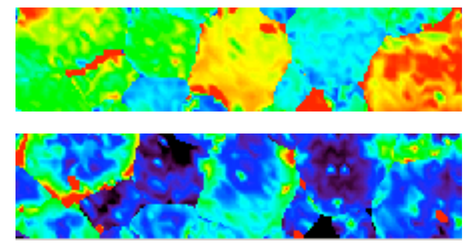
Maximum resolved shear stress and dislocation density maps of a NiTi alloy

Crystalline species spatial distribution

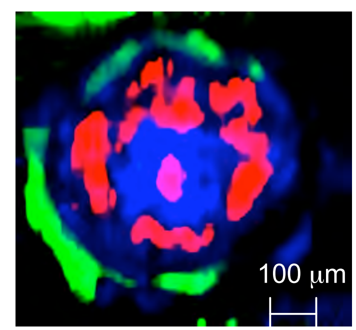

R: lithiophorite

G: goethite

B: Birnessite

Mineralogical species distribution map of a ferromanganese soil nodule

Critical problems associated with the use of an X-ray microbeam

Sphere of confusion — No sphere of confusion

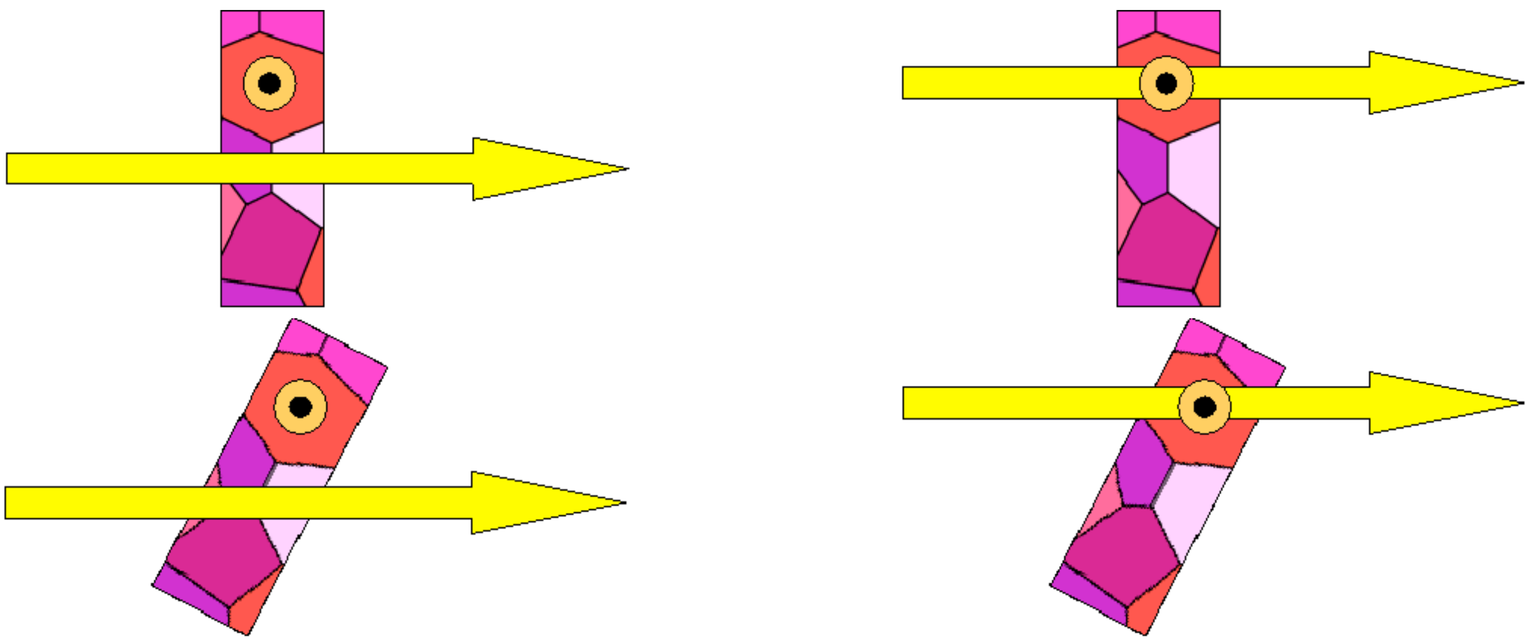

The diffracted volume is different for every sample tilt regardless of the position of the center of rotation of the goniometer => sample rotation must be avoided

Schematic layout of the X-ray Microdiffraction Beamline (7.3.3.) at the ALS

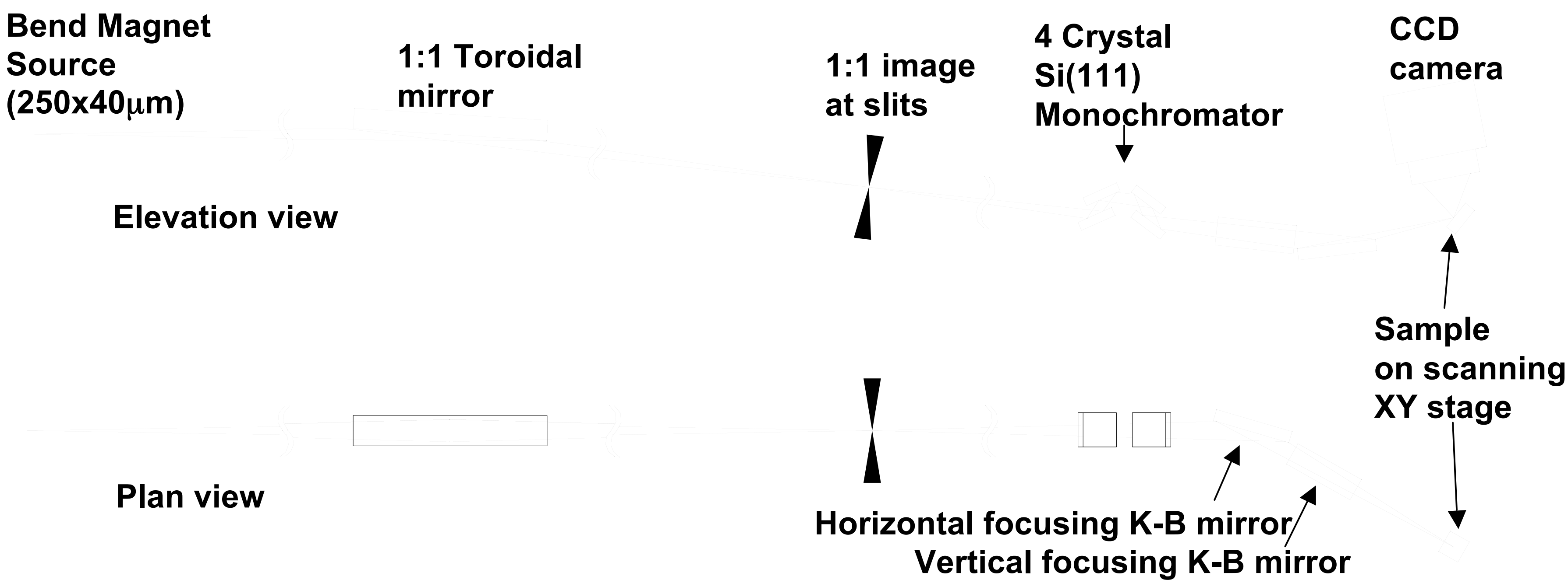

Beam size on sample: 0.8x0.8 μm^2

Photon energy range: 5-14 keV

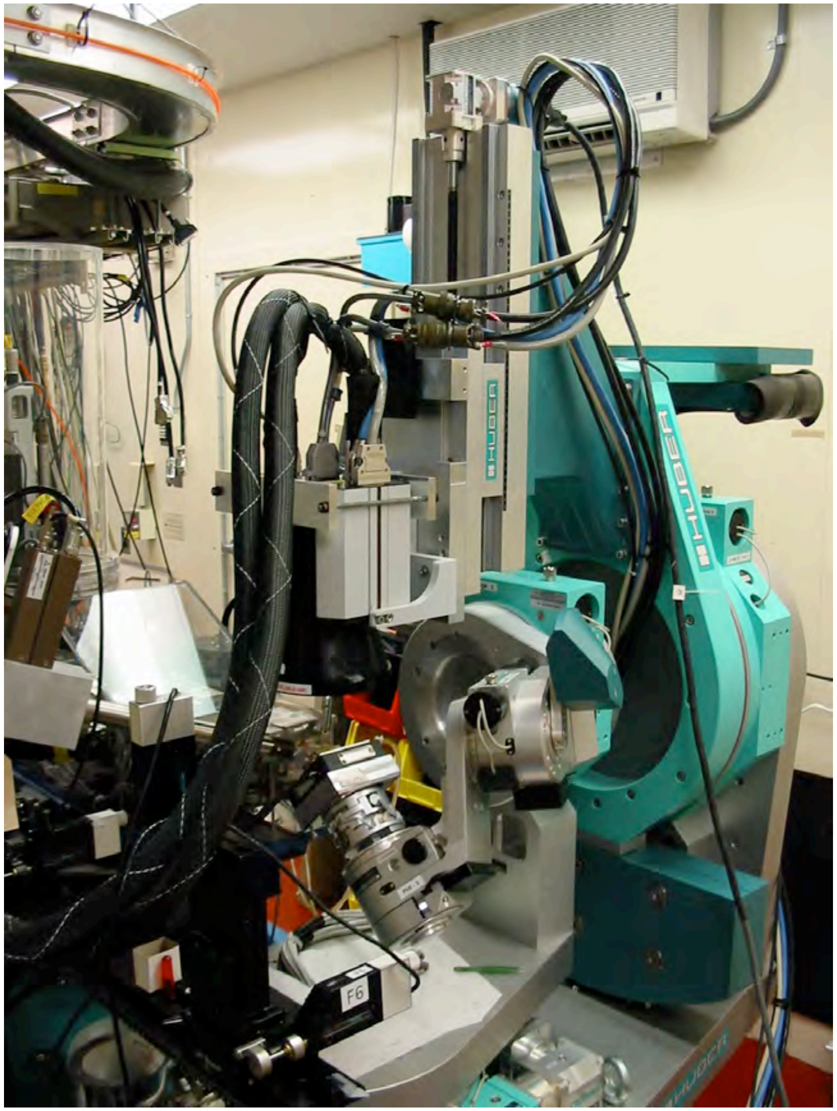

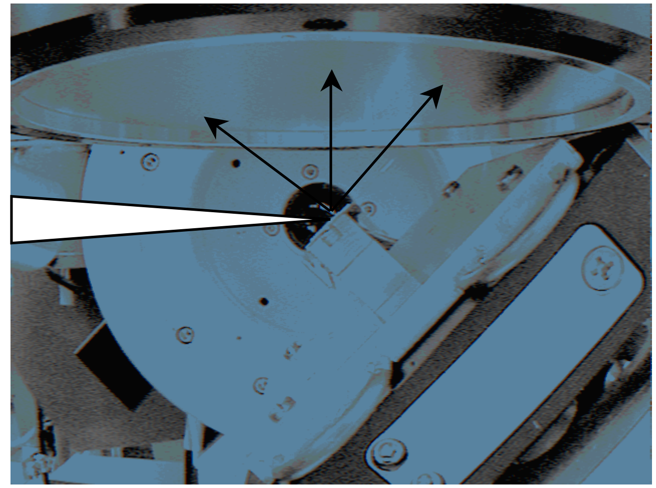

- Huber 6-circle diffractometer
- Bruker SMART 6000 CCD (9x9 cm^2 active area)
- Si(Li) EG&G ORTEC detector
- Sample mounted on a XYZ Huber stage and a PI Piezo stage
- Heating/Cooling stage

White beam X-ray microdiffraction methodology

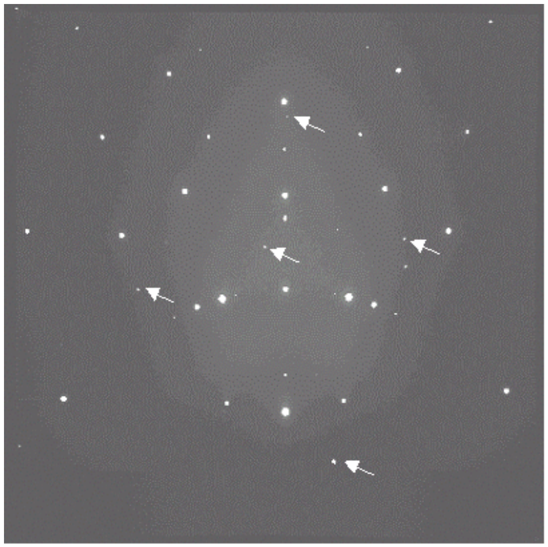

White beam (Laue) diffraction pattern of an Al(Cu) interconnect. The brighter spots are from Si wafer.

The sample is scanned under a white X-ray microbeam. At each step a diffraction (Laue) pattern is collected with the CCD detector. A preliminar X-ray fluorescence scan can be used to precisely locate the region of interest

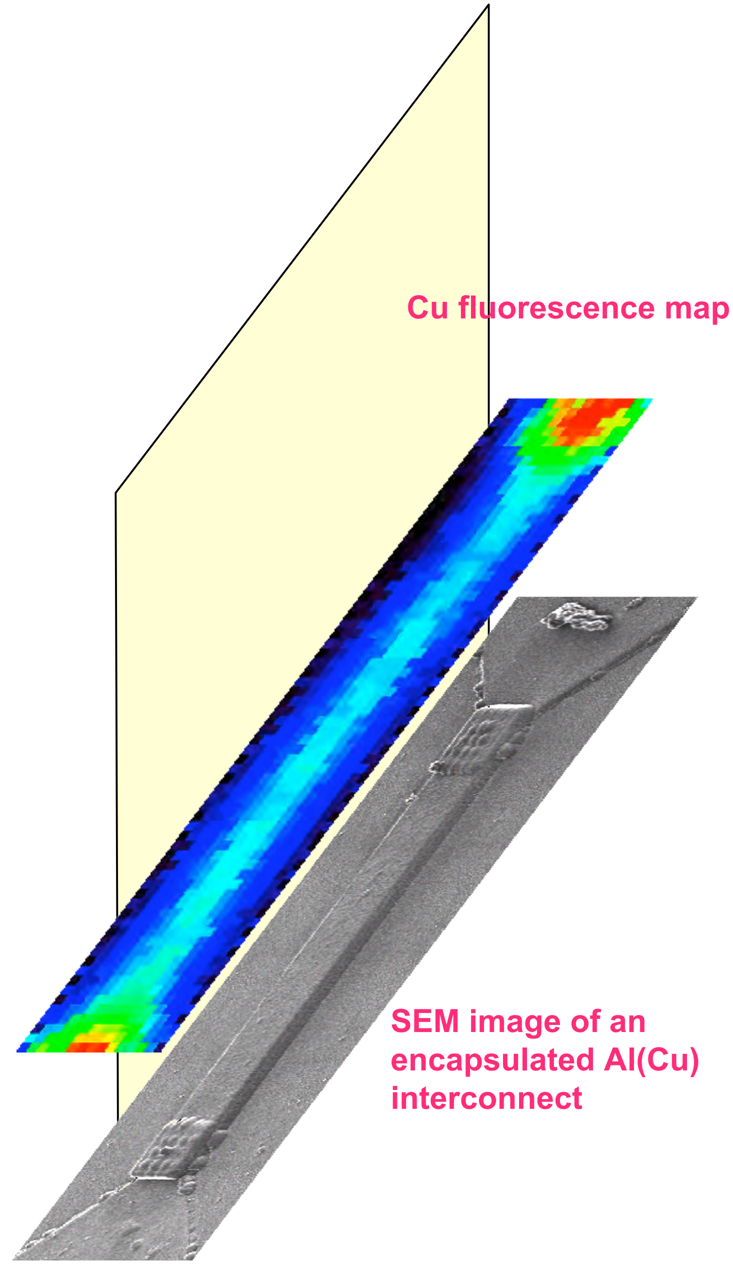

White beam X-ray microdiffraction methodology

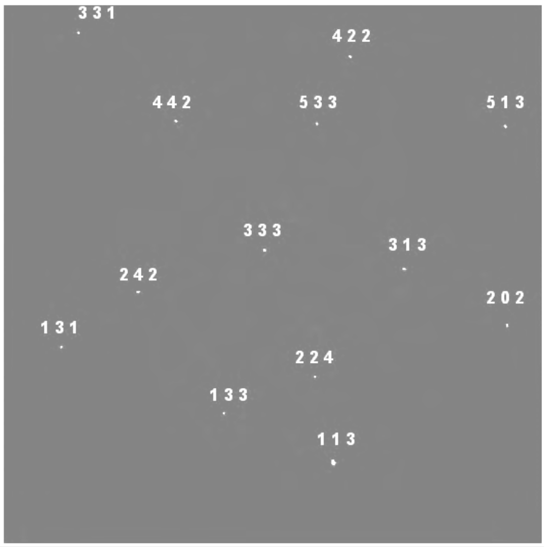

Si spots from the wafer have been digitally removed. The remaining Al spots are indexed.

The indexation of the Laue patterns provide the crystal orientation matrix of the area illuminated by the X-ray microbeam. The analysis of the entire scan gives the grain orientation map of the sample.

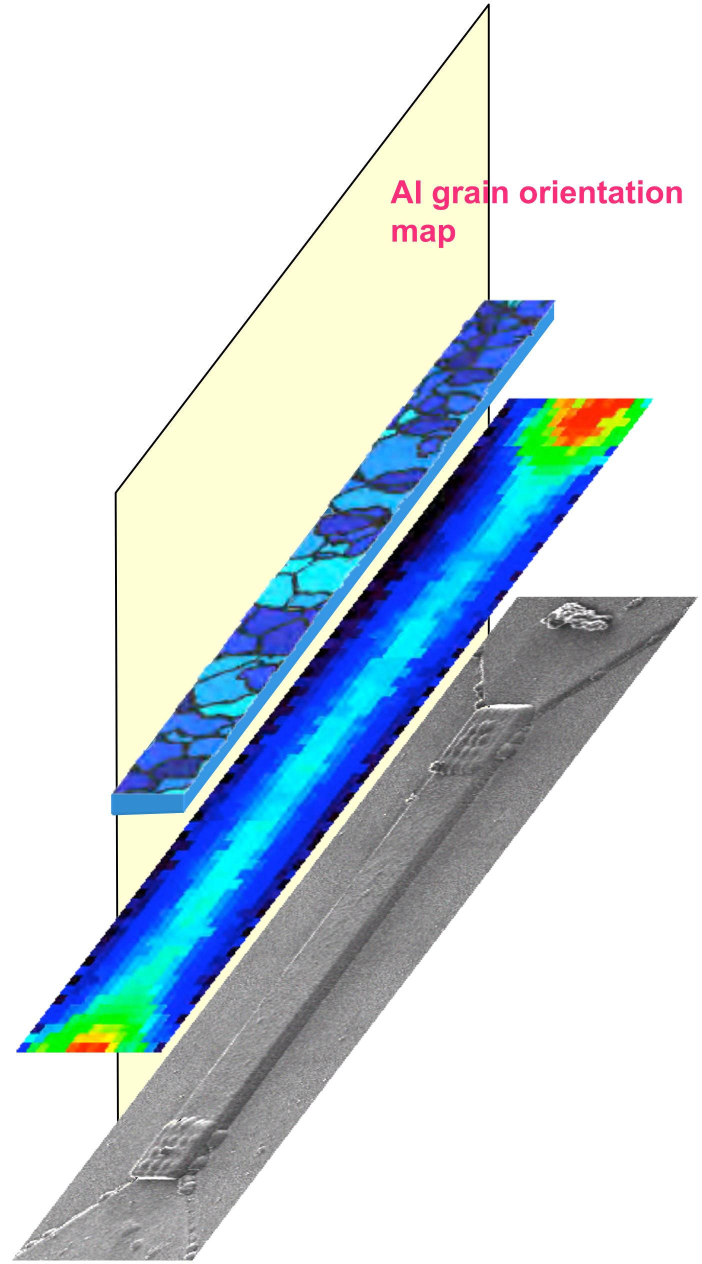

White beam X-ray microdiffraction methodology

Deviations of the Laue peaks positions from their "unstrained" positions provide the distortional strain tensor.

$$\varepsilon_{ij} = \begin{bmatrix} \varepsilon'_{11} & \varepsilon_{12} & \varepsilon_{13} \\ \varepsilon_{21} & \varepsilon'_{22} & \varepsilon_{23} \\ \varepsilon_{31} & \varepsilon_{32} & \varepsilon'_{33} \end{bmatrix} + \begin{bmatrix} \delta & 0 & 0 \\ 0 & \delta & 0 \\ 0 & 0 & \delta \end{bmatrix} \qquad \delta = \frac{\varepsilon_{11} + \varepsilon_{22} + \varepsilon_{33}}{3}$$

Measured from deviations in crystal Laue pattern (Using White Beam)	Measured from energy of Laue spot (Using Monochromatic beam)

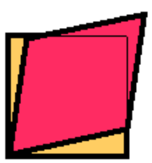

Shear strain
$\varepsilon_{12} = \varepsilon_{21}$

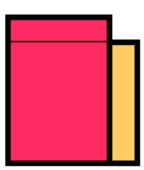

Tensile/compressive distortional strain
$\varepsilon'_{11}, \varepsilon'_{22}$

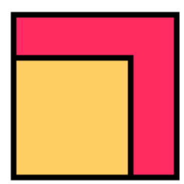

Dilatational strain
δ

- Stress tensor: $\sigma_{ij} = C_{ijkl}\, \varepsilon_{kl}$

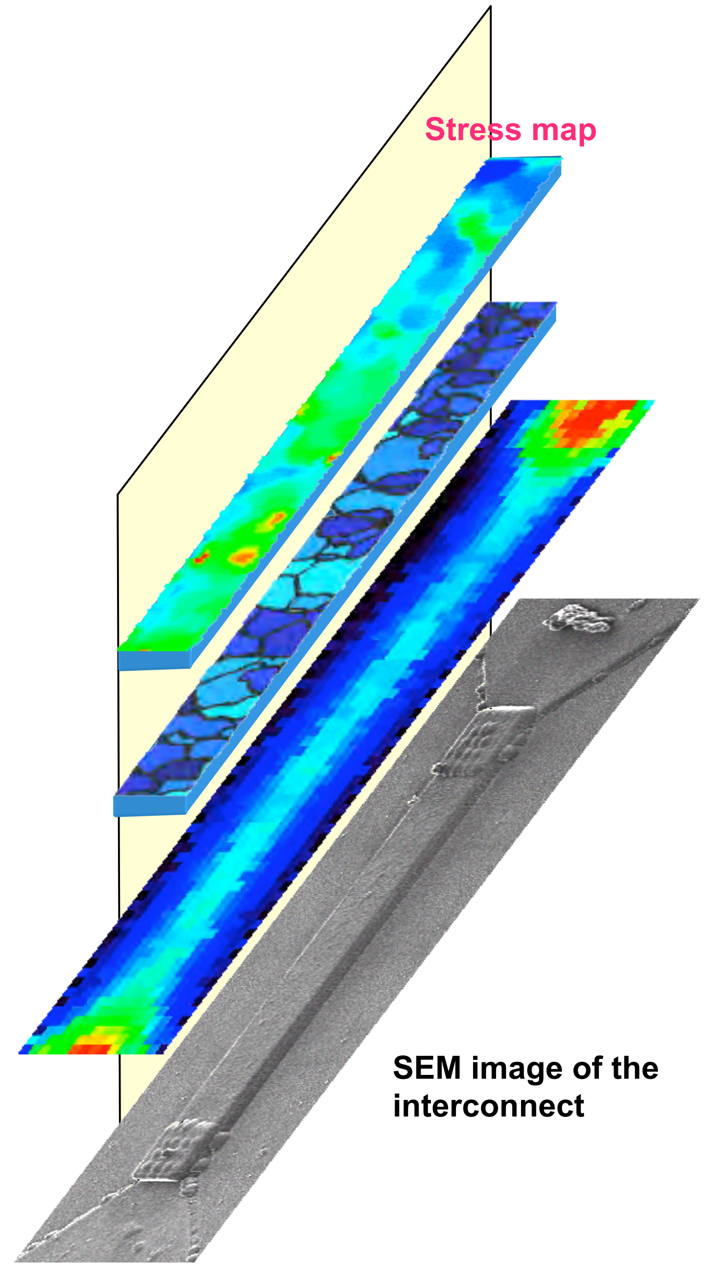

White beam X-ray microdiffraction methodology

Peak shapes provides information on plastic deformation and dislocation distribution in the diffracted volume.

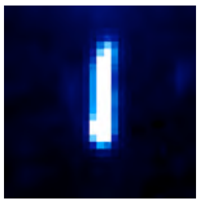

$$\rho = \frac{1}{Rb}$$

Cahn-Nye Relation

Pure bending

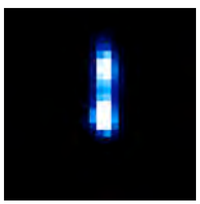

$$\tan è = \frac{b}{L}$$

Subgrain boundary

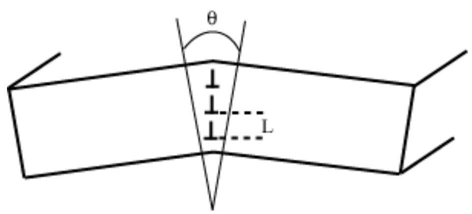

(224)

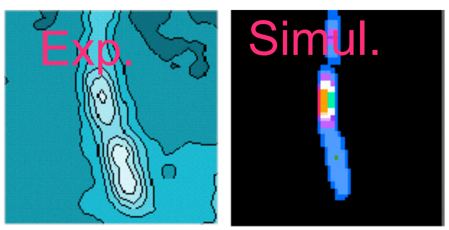

b=[0-11];τ =[-211]

b=[110];τ =[-112]

Burgers vector and dislocation line directions can be derived from the shape of the Laue reflections (Barabash et al., 2002 and 2003)

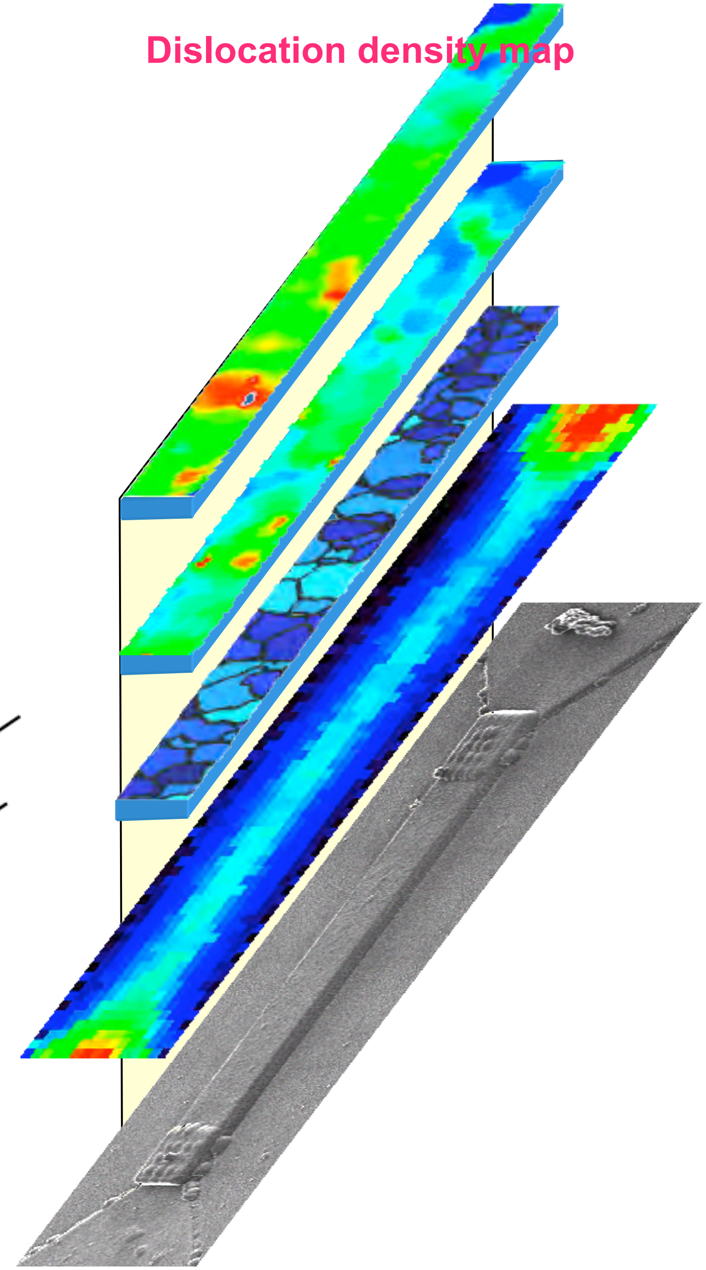

Applications of X-Ray Microdiffraction

Measuring Mechanical properties of materials at microscopic level Materials properties such as strength and resistance to fatigue are highly dependant of the microstructure. Scanning X-Ray Microdiffraction is a technique which can measure local stress variations between grains and inside individual grains, helping us understand the mechanical properties of materials at this critical length scale.

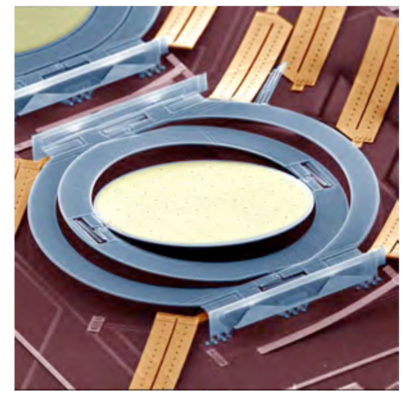

Measuring Mechanical properties of very small devices In microelectronics and related industries, the dimensions of the constitutive devices have sizes ranging from a few microns to submicron. Confinement made their mechanical properties drastically different from those of bulk materials. X-ray Microdiffraction provides a way to measure local characteristics such as texture and stress on the individual devices offering an experimental counterparts to computer simulations.

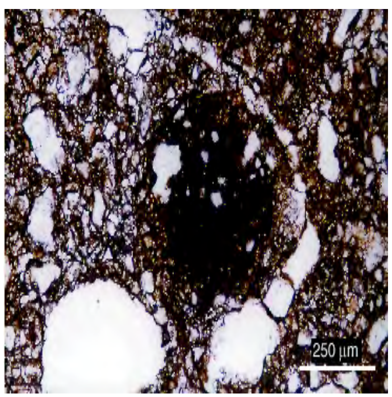

Characterizing complex and heterogeneous materials Samples like soils are highly complex and constitute a challenge for spatially resolved characterization. X-ray microdiffraction allows for a non invasive structural identification of small amounts of phases embedded in a heterogeneous matrix.

Electromigration-induced plasticity in Al(Cu) interconnects

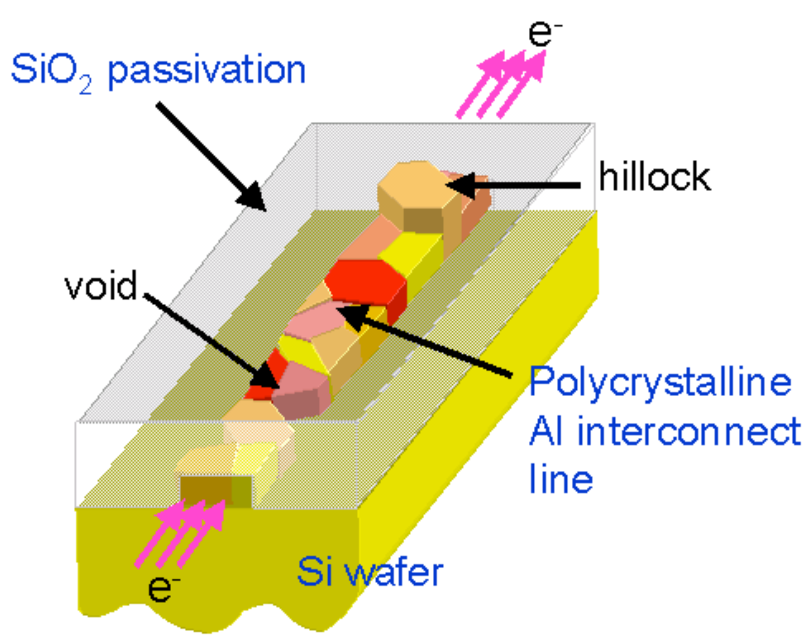

Inside a microchip, metal Interconnect lines are subject to extremely high (~ 10^6 A/cm^2) current density sufficient for the electron wind to physically displace the constitutive atoms of the lines (electromigration).

Depletion of atoms could cause voids formation, accumulation of atoms could lead to hillocks and passivation crack.

Electromigration-induced failure constitutes a severe reliability problem in the microelectronic industry.

X-ray microdiffraction has the ability to probe individual grain of the interconnect below the passivation layer and monitor structural changes (deformation) as the current is running in the line.

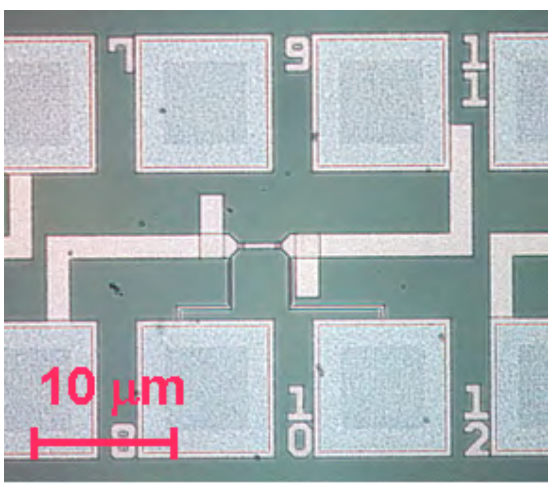

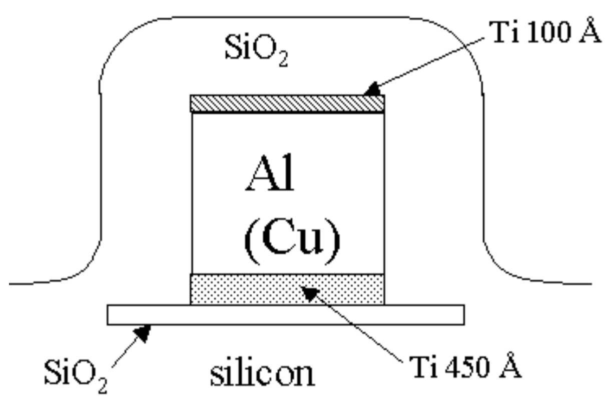

Sample: The interconnect test structure is a 30 μm long, 4.1 μm wide and 0.75 μm thick Al(0.5wt%Cu) line passivated under a 0.7 μm thick SiO_2 cap.

Electromigration-induced plasticity in Al(Cu) interconnects

An accelerated electromigration test experiment was performed at 205 °C on a 30 μm long, 4.1 μm wide and 0.75 μm thick Al(0.5wt%Cu) passivated line

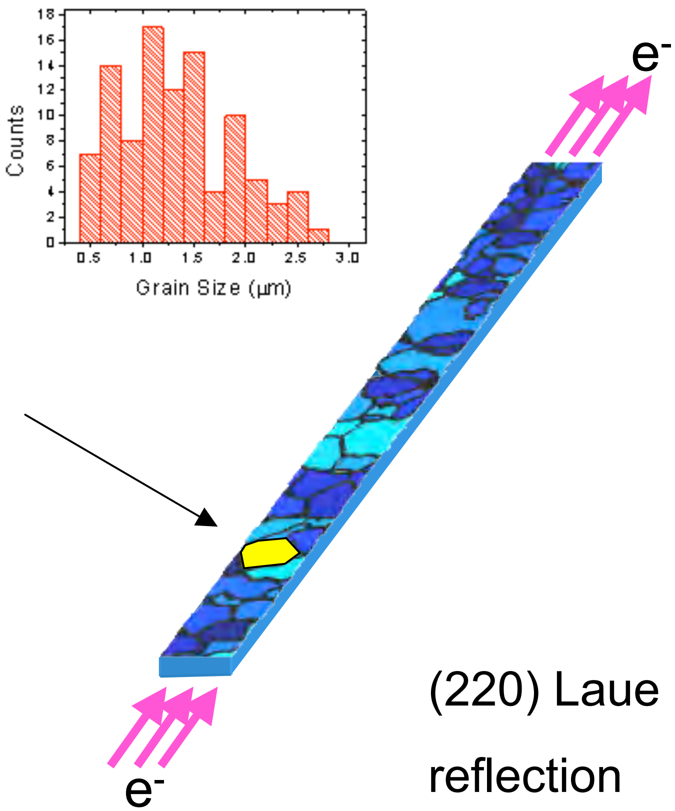

(220) Laue reflection

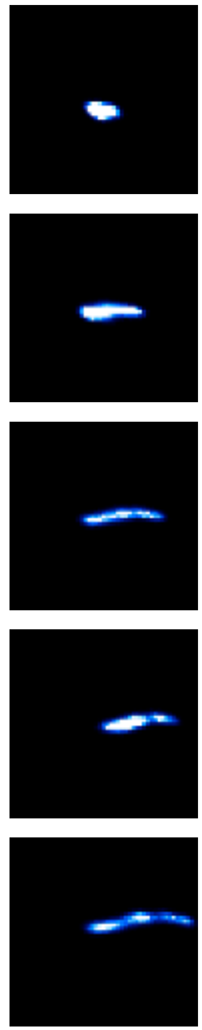

J= 0 A/cm^2
t= 0 h

J= +10^6 A/cm^2
t= 13.55 h

J= +10^6 A/cm^2
t= 19.45 h

J= -10^6 A/cm^2
t= 36.15 h

J= -10^6 A/cm^2
t= 46.30 h

The line was repeatedly raster-scanned with X-ray microdiffraction during the test.

The recorded Laue diffraction patterns of individual grains showed streaking of the reflections in a direction transverse to the current flow.

The amount of streaking depends on the position on the line and the size of the grain and evolves over time as electromigration is going on

In the case of large grains, the streaking is important and peak splitting into several maxima is observed indicating subgrain formation

Electromigration-induced plasticity in Al(Cu) interconnects

A small grain exhibits less streaking of the reflections. Peak shifting indicates grain rotation across the line width

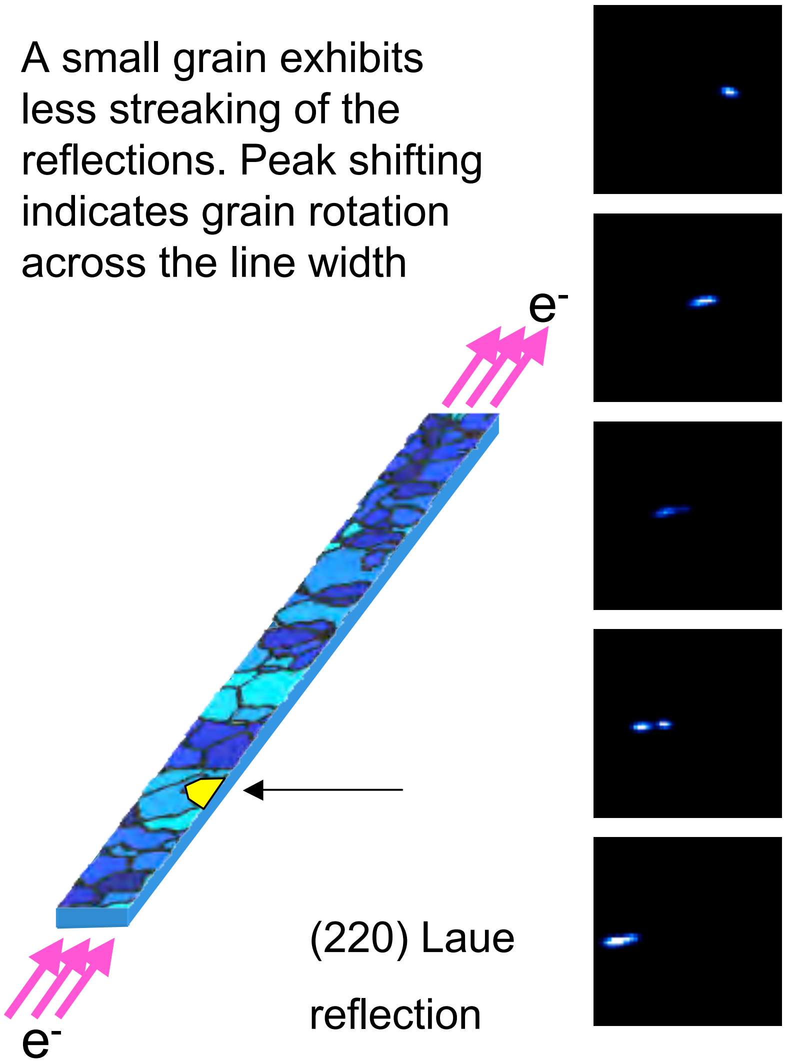

The rotation direction is opposite for grains situated at opposite side of the line width

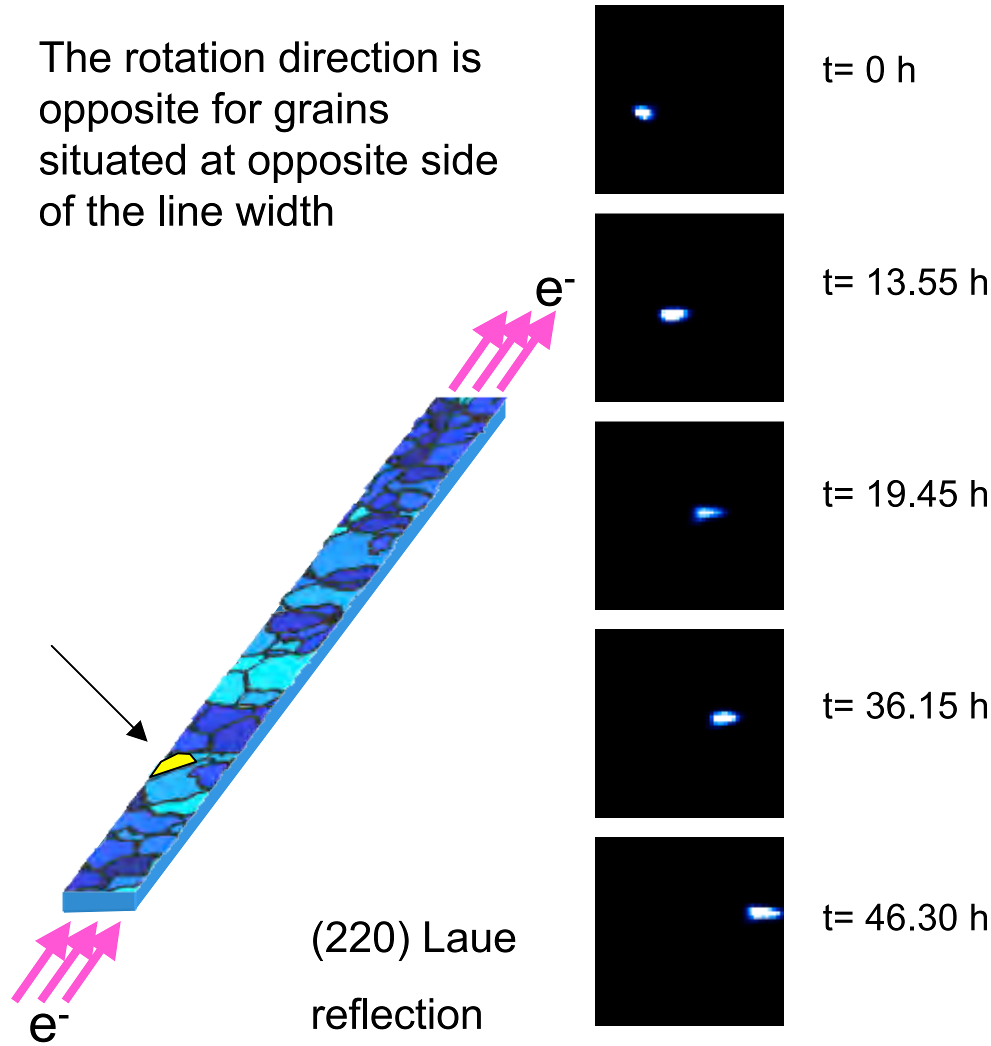

Electromigration-induced plasticity in Al(Cu) interconnects

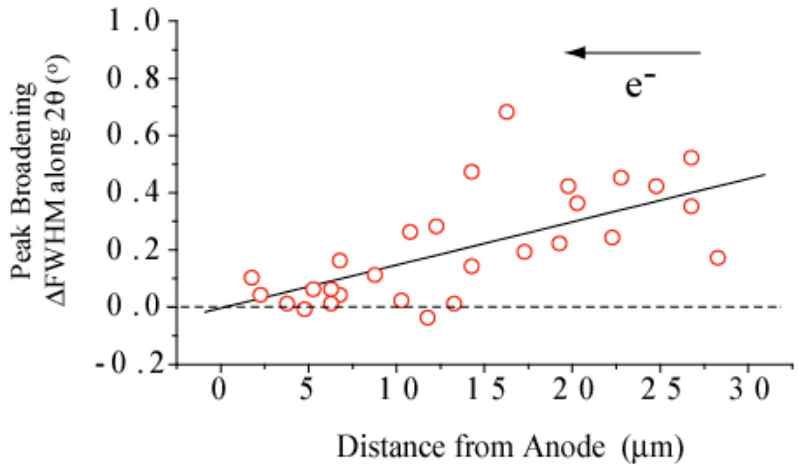

A gradient of grain deformation is established during the early stage of electromigration as indicated by the position dependence of the amount of peak streaking. Grains closer to the cathode tends to be more deformed.

A gradient of grain rotation is established as well with grains on opposite sides of the line width rotating in opposite direction. Rotation is more pronounced at the cathode end.

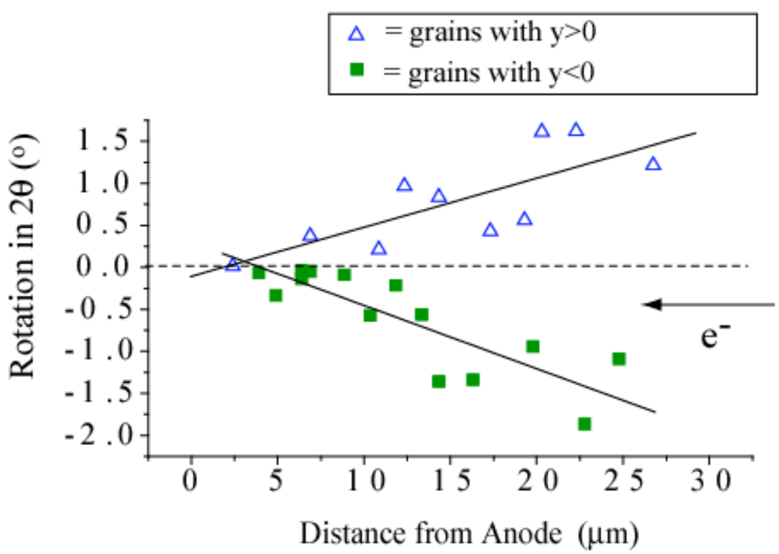

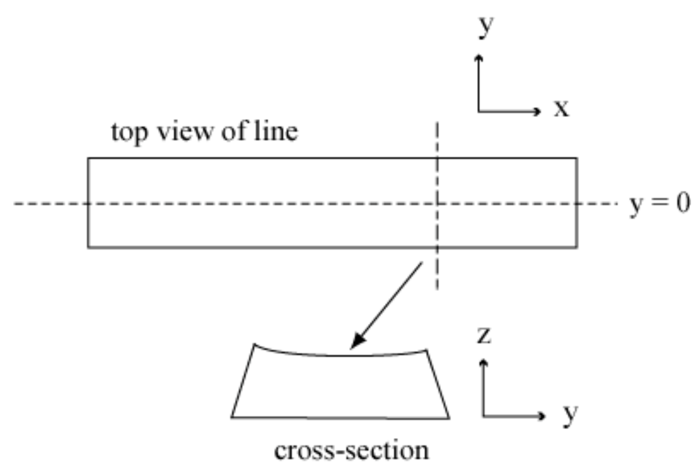

Electromigration-induced plasticity in Al(Cu) interconnects

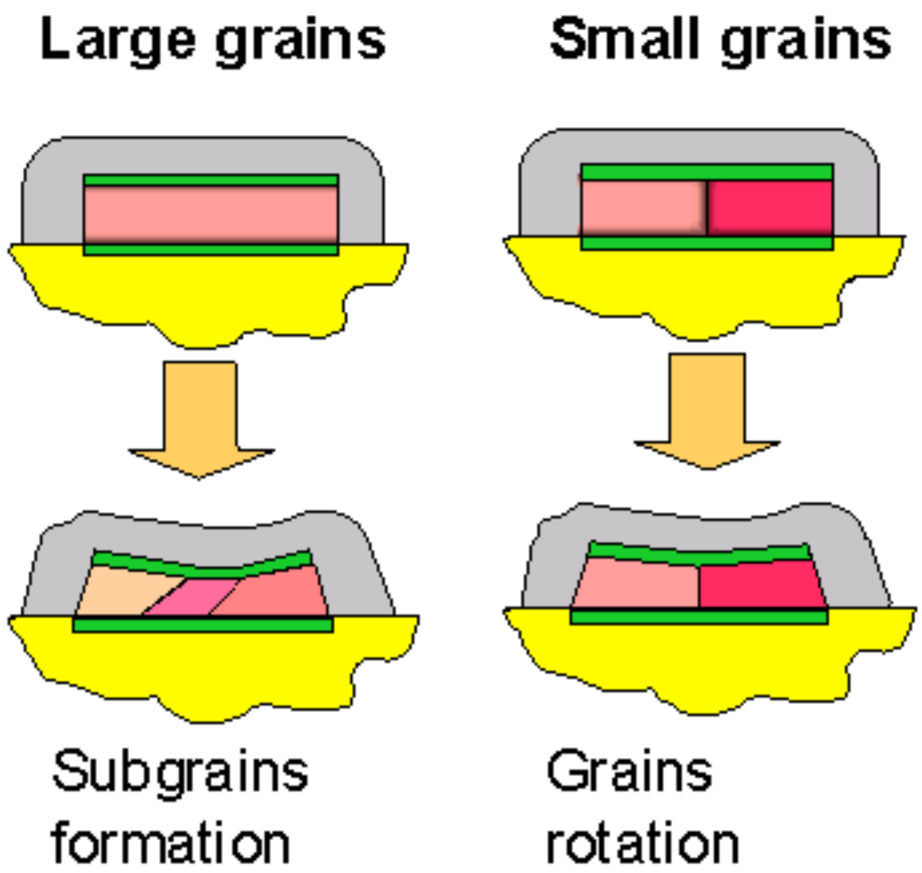

Model of electromigration-induced plastic deformation derived from the X-ray microdiffraction data

Materials travel along grain boundaries and interfaces => concentration of vacancies at the cathode end leading to tensile strain

Due to higher compliance of the passivation layer, the tensile stress in the upper half of the line is relieved by bending (subgrains formation, grain rotations).

N. Tamura et al., Appl. Phys. Lett. 80 (2002) 3724
B.C. Valek et al., Appl. Phys. Lett. 81 (2002) 4168
B.C. Valek et al., J. Appl. Phys. (2003) in press

Electromigration-induced plasticity in Al(Cu) interconnects

Why is plastic deformation only observed towards the cathode end?

During EM, Cu migrates from the cathode to the anode end where Al_2Cu precipitates can be observed.

The cathode becomes Cu depleted and therefore “softer” than the anode end and will deform first.

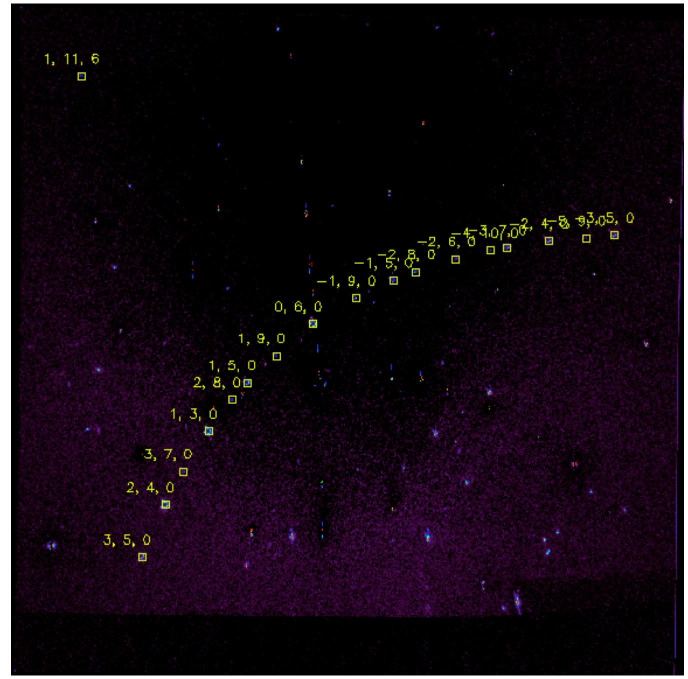

Al2Cu precipitate Laue pattern

in Al(Cu) line after EM

Presentation plan

1. Why use synchrotron radiation?
2. Single crystal diffraction
    1. Polychromatic
    2. Monochromatic
3. Powder diffraction
    1. Monochromatic
    2. Polychromatic

Experimental Techniques: Beamline

CHARACTERISTICS

- High flux
- Tunable, monochromatic
- Optimized for small molecule crystallography.

Top view of BL.11.3.1 components.

BL.11.3.1 is mounted on a regular ALS bending magnet.

Energy range	**6-17 keV (0.73-2.07 Å)**
Beam size	**280 x90 μm down to 100 μm^2**
Flux	**10^{10} ph/s at sample location**
Spatial resolution	**100 μm**
Sample requirements	**Solid (small crystal or powder), liquid (in capillary or cells)**

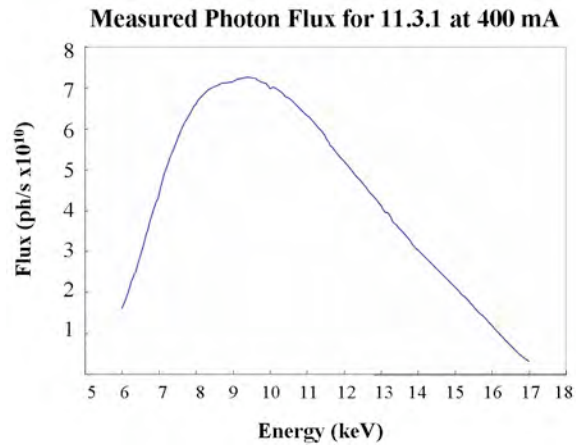

Experimental Techniques: Beamline

MONOCHROMATOR

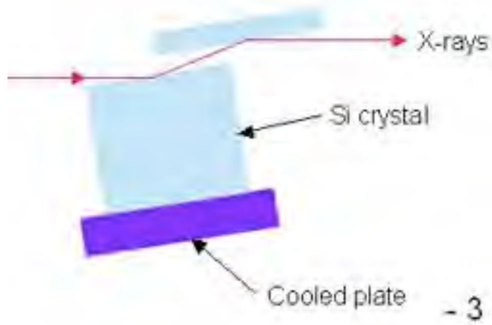

Channel-cut Si<111>
Crystal

- 3 mm separation (5.9 mm offset)
- second surface offset .28 deg gives only 24 μm motion from 9-16 keV
- power is about 14 watts at 400 mA

Si<111> Channel-Cut Monochromator

Internal View

External View

advanced light source ESG experimental systems group

Experimental Techniques: End-Station

- **Platinum 200 CCD detector (Fairchild), four-port readout, coupled to a 20 cm diameter fiber-taper optic.**

- **Equipped with a 3 circle, fixed-Chi (54.7°) Bruker goniometer.**

- **Typical exposure times:**
- for single crystal experiments: 0.5 to 5 s/frame.
- for powder XRD: 120s/frame.

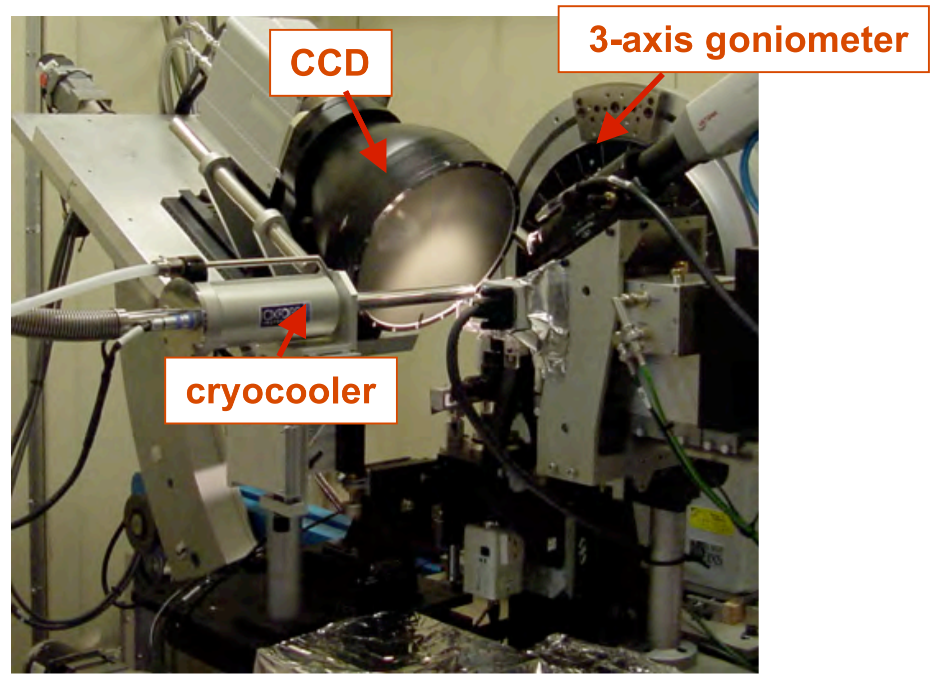

11.3.1 Endstation- Small Molecule Crystallography Set-up

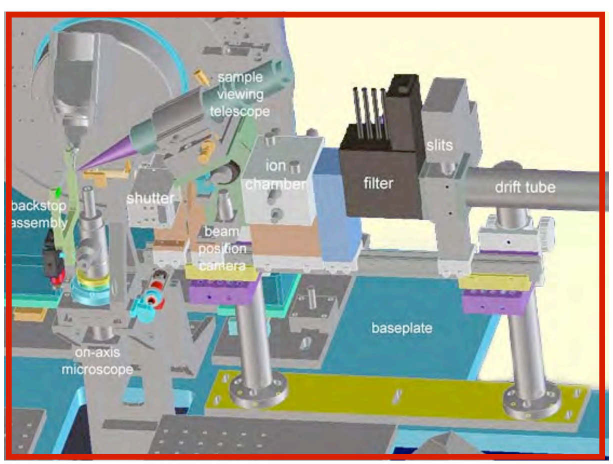

- **The Bruker APEX2 software is used to resolve compound structures (Single crystal XRD).**

- **Smart or Fit 2D or Xmas are used to analyze the powder and high pressure XRD data.**

Diffraction pattern

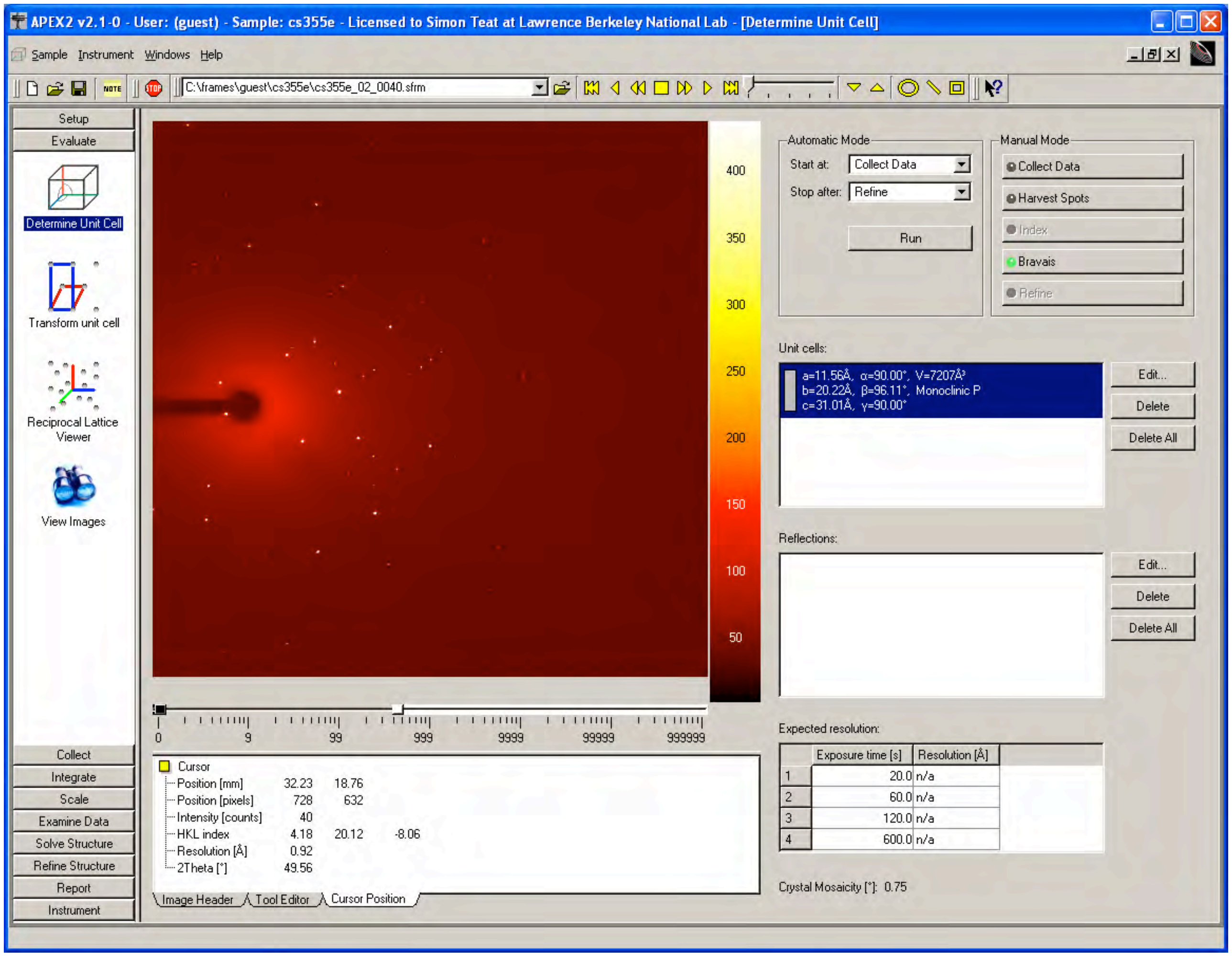

Diffraction pattern with reflection predications from indexing

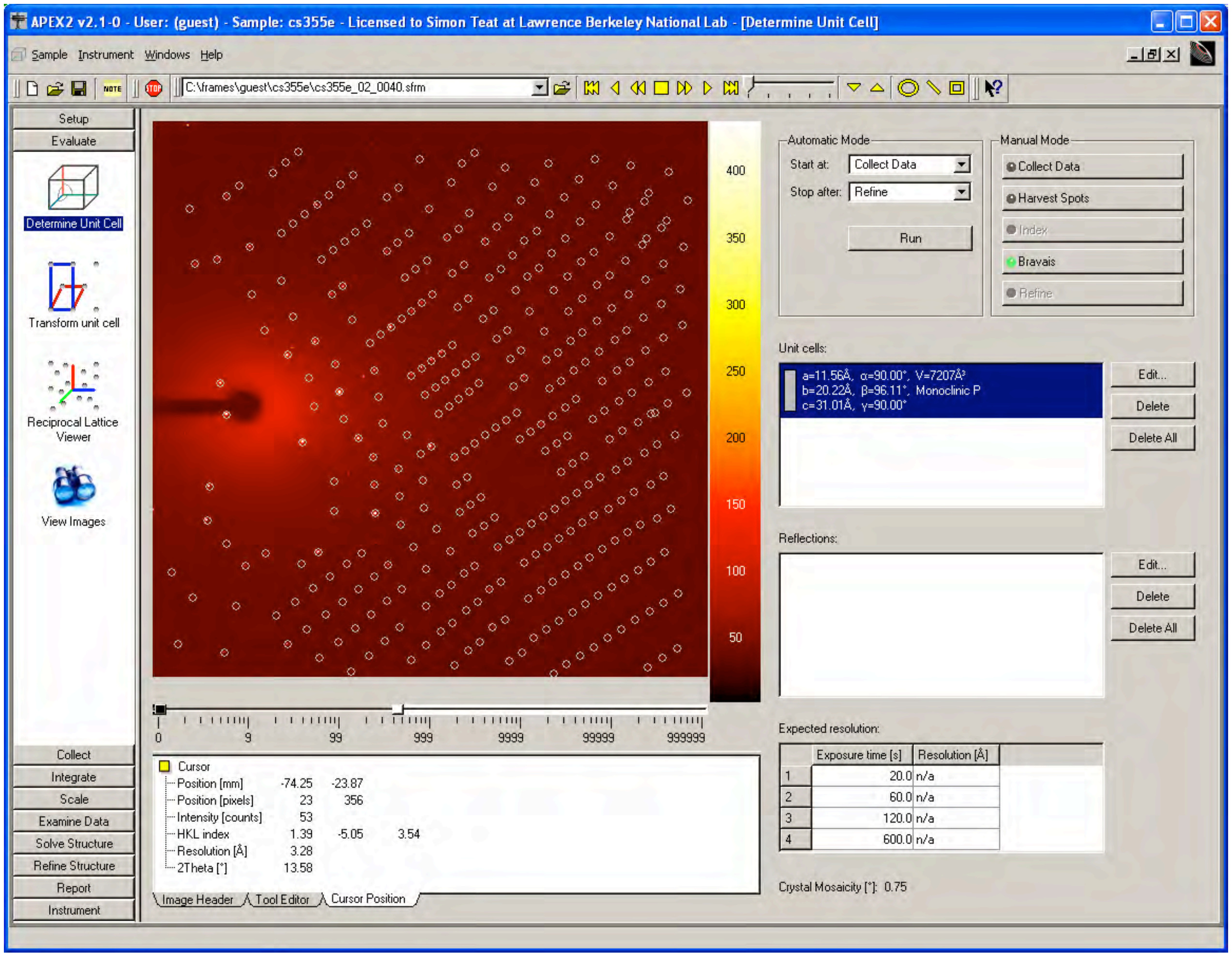

Application: Small molecule XRD

EXAMPLE 2 : FIRST SINGLE CRYSTAL XRD ANALYSIS OF A Pu (IV) HYDROXYPYRIDONATE COMPLEX

MOTIVATION

Many of the radioactive wastes present at DOE long-term storage sites are large mixtures of metals with actinides in solution. The selective removal of the actinides, Cs, and Sr, the predominant radioactive elements in these waste streams, would concentrate the volume of high-level waste and reduce the amounts requiring disposal in a geological repository.

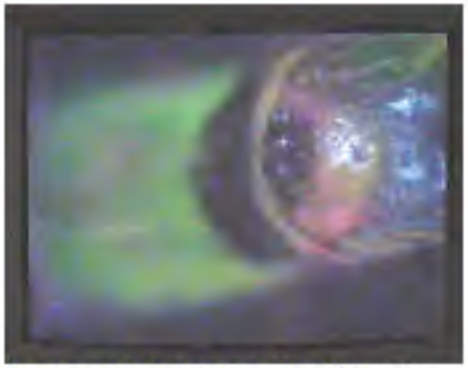

Pu(IV) - 5LIO(ME-3,2-HOPO) – The purple crystal (magnified 20x) diffracts green light - taken at the Advanced Light Source beamline 11.3.1.

A. E. V. Gorden, D.K. Shuh, B. E. F. Tiedemann, R. E. Wilson, J. Xu, K.N. Raymond, University of California and LBNL

Back to Applications

Application: Small molecule XRD

EXAMPLE 2 : FIRST SINGLE CRYSTAL XRD ANALYSIS OF A Pu (IV) HYDROXYPYRIDONATE COMPLEX

- Similar properties of Fe(III) and Pu(IV) inspired actinide extractants based on hydroxypyridinone (HOPO) chelating units like those found in naturally occurring Fe(III) selective extractants.
- A detailed evaluation of the structure of actinide complexes is important to the design of new selective ligands.
- Only 23 Pu complexes have been reported to the Cambridge Crystallographic Database!
- The Pu(IV)-[5LIO(Me-3,2-HOPO)]$_2$ complex is the first in a series to be characterized and will provide a basis for the modeling and design of future systems, and for EXAFS.

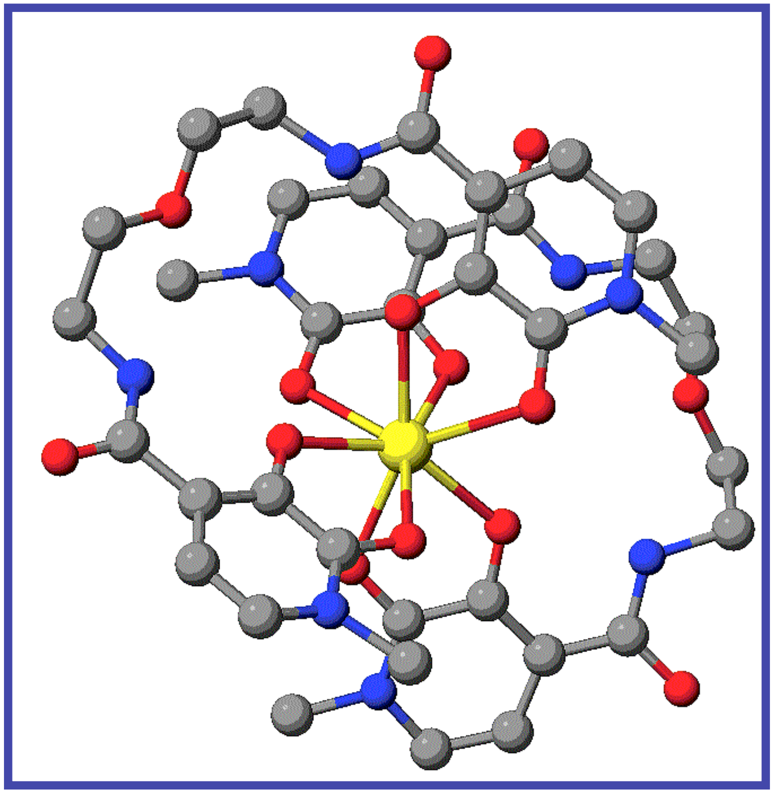

Pu1-Ophenolic 2.307(31) Å
Pu1-Oamide 2.401(23) Å
Average Bite Angle 67.3(4)º

A. E. V. Gorden, D.K. Shuh, B. E. F. Tiedemann, R. E. Wilson, J. Xu, K.N. Raymond, University of California and LBNL

Back to Applications

Application: Small molecule XRD

EXAMPLE 3 : FIRST SINGLE CRYSTAL XRD ANALYSIS OF A Pu (IV) HYDROXYPYRIDONATE COMPLEX

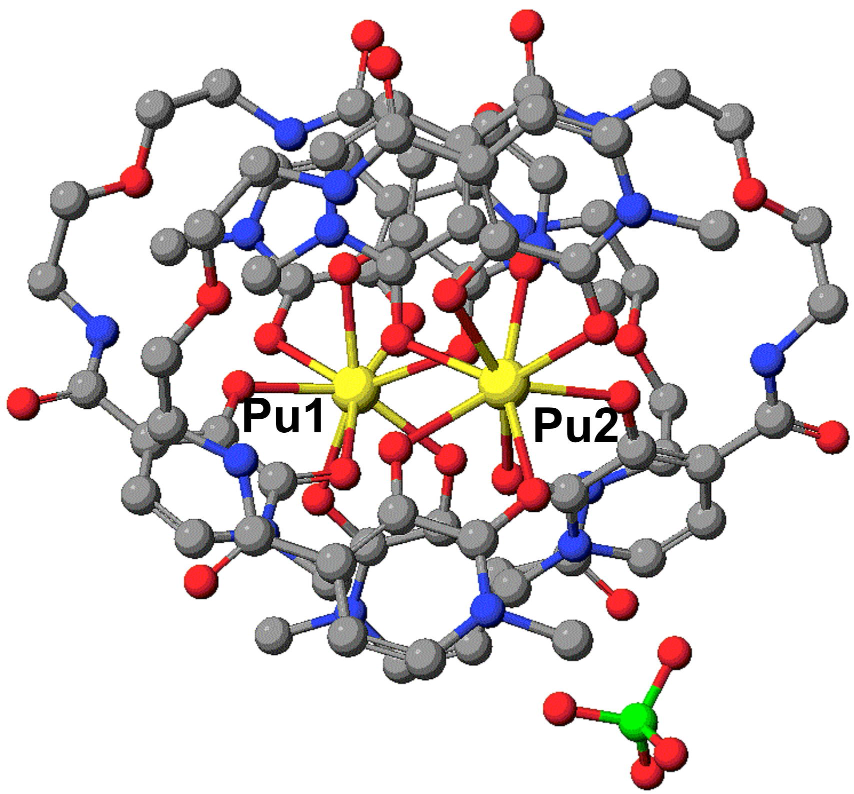

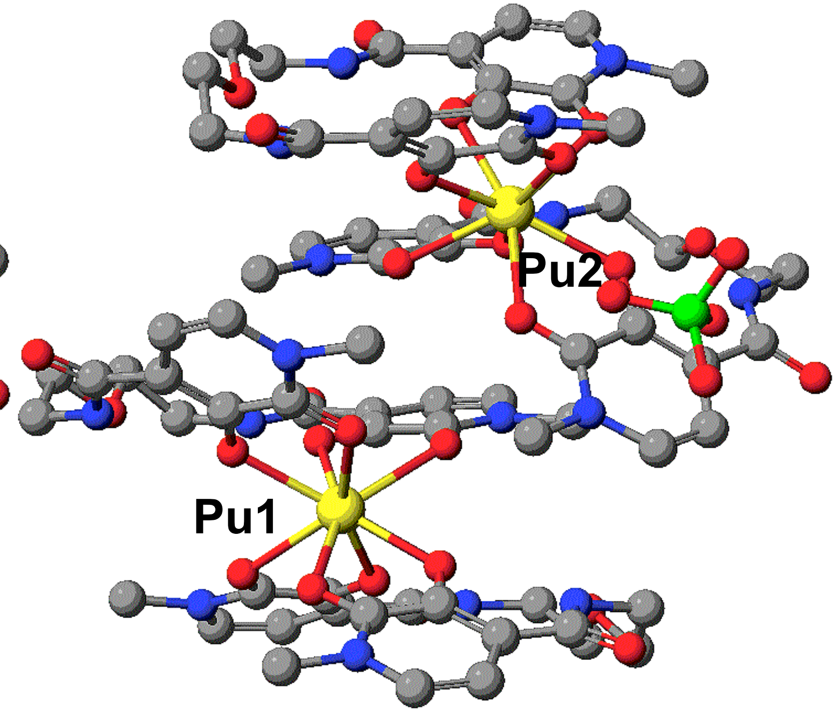

Pu(5LIO-Me-3,2-HOPO)$_2$

A. E. V. Gorden, D.K. Shuh, B. E. F. Tiedemann, R. E. Wilson, J. Xu, K.N. Raymond, University of California and LBNL

Application: Small molecule XRD

EXAMPLE 3 : FIRST SINGLE CRYSTAL XRD ANALYSIS OF A Pu (IV) HYDROXYPYRIDONATE COMPLEX

Pu(5LIO-Me-3,2-HOPO)$_2$

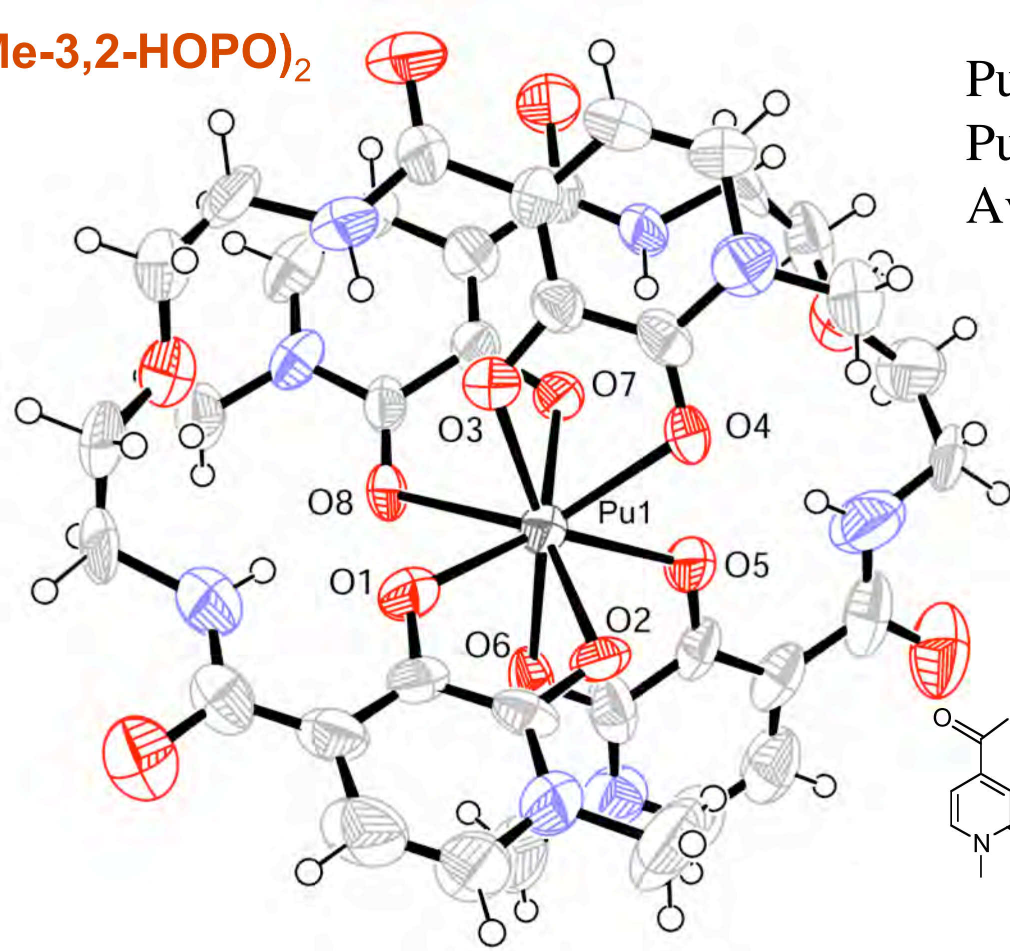

$Pu1\text{-}O_{phenolic}$ 2.307(31) Å

$Pu1\text{-}O_{amide}$ 2.401(23) Å

Average Bite Angle 67.3(4)º

Orthorhombic, Z=4	
Pna21 space group	
Temperature 298K	
0.50x0.50x 0.70 (mm)	
63115 reflections	
16280 independent	
R(int)	0.0938
R1	0.0629
wR2	0.1624

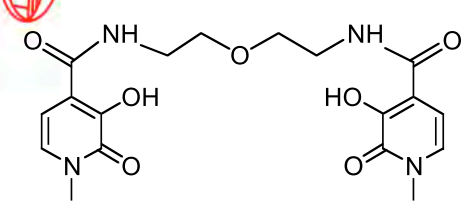

5LIO(Me-3,2-HOPO)

A. E. V. Gorden, D.K. Shuh, B. E. F. Tiedemann, R. E. Wilson, J. Xu, K.N. Raymond, University of California and LBNL

Back to Applications

Application: Small molecule XRD

EXAMPLE 4 : FIRST SINGLE CRYSTAL XRD ANALYSIS OF A Np (V) COMPLEX

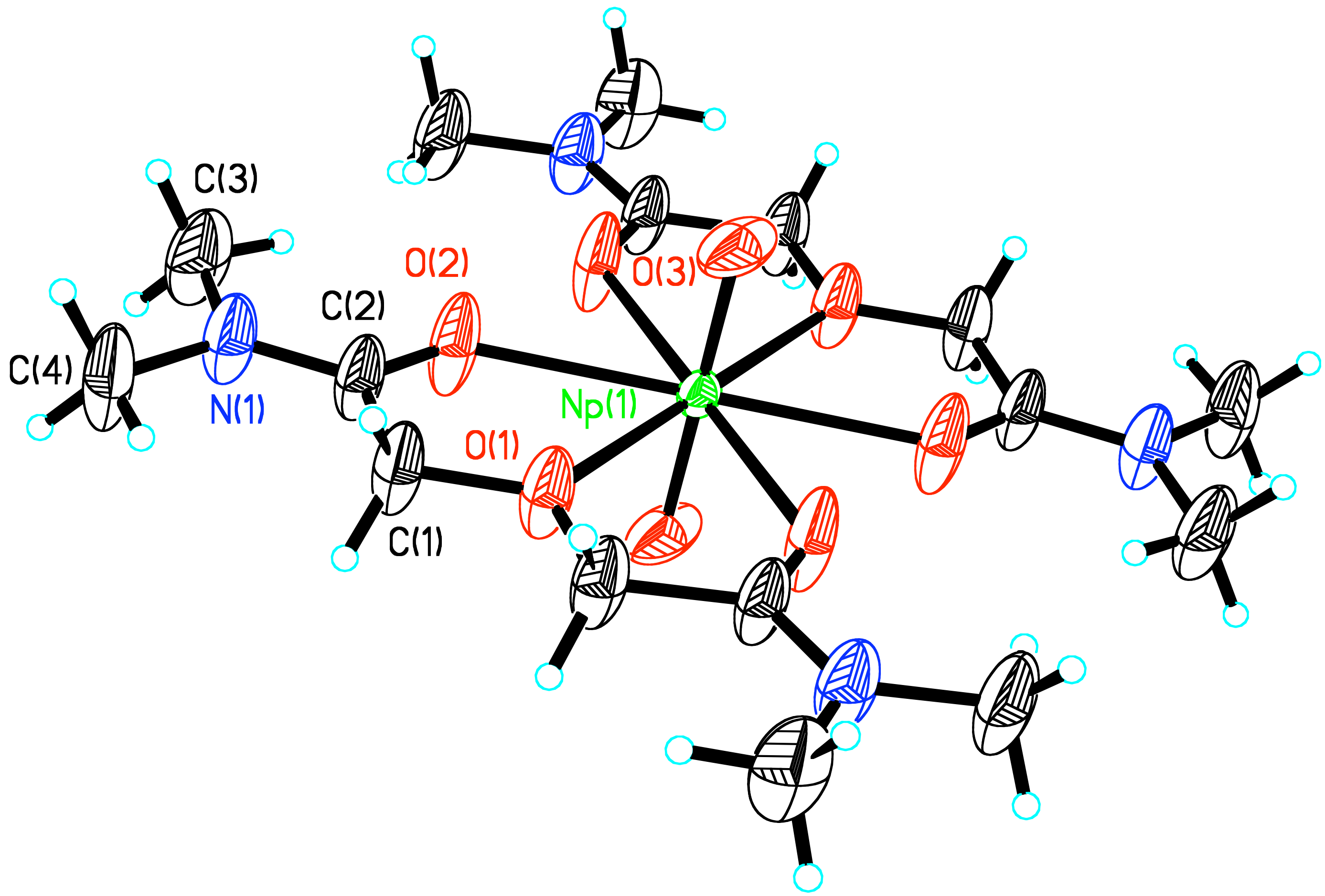

Structure of $NpO_2(L)_2ClO_4$(cr), where L stands for N,N,N',N'-tetramethyl-3-oxa-glutaramide. The ClO_4^- anion is not shown for clarity (G. Tian, J. Xu, L. Rao, *Angew. Chem. Int. Ed.* 44, 6200, 2005.)

Application: Small molecule XRD

EXAMPLE 4 : FIRST SINGLE CRYSTAL XRD ANALYSIS OF A Np (V) COMPLEX

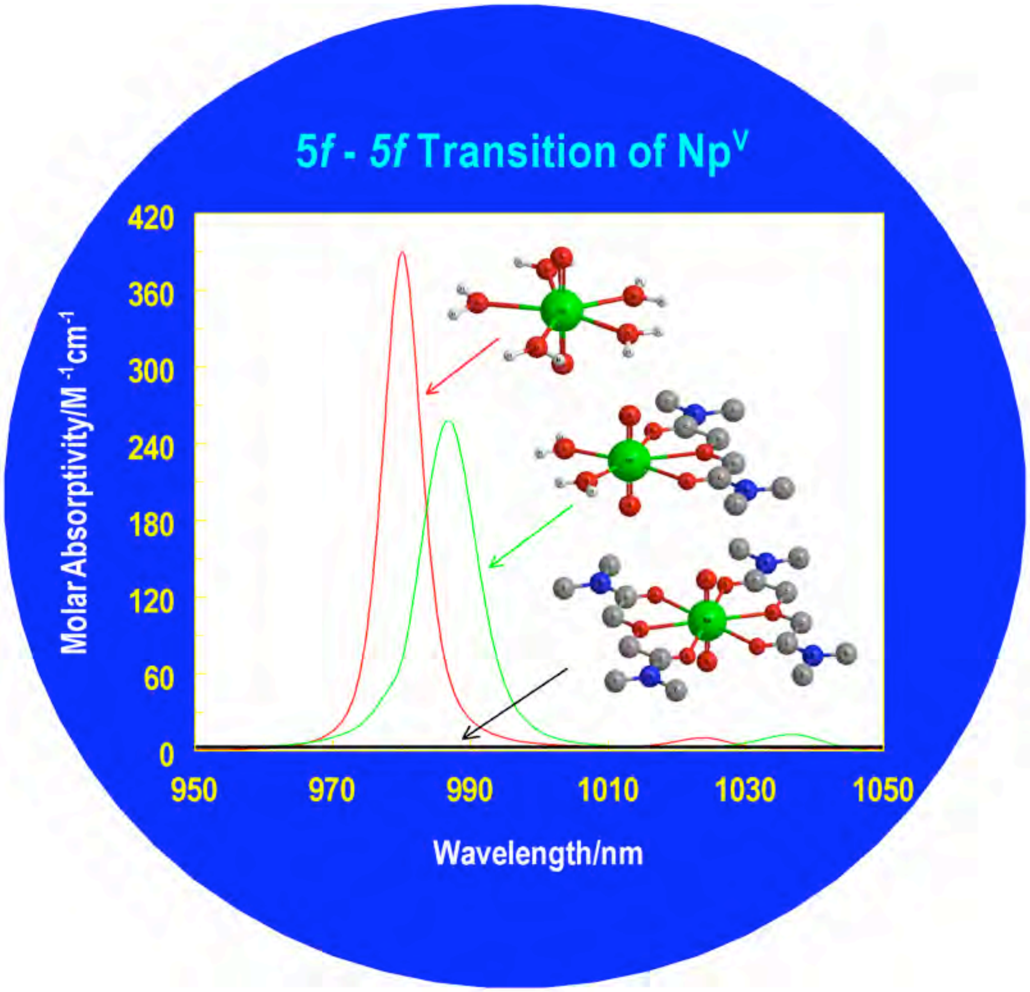

Atomic symbols: Np (green), oxygen (red), nitrogen (blue), carbon (charcoal), hydrogen (gray, small).

The structure of $NpO_2(L)_2ClO_4$(cr), where L stands for N,N,N',N'-tetramethyl-3-oxa-glutaramide, was identified at the Advanced Light Source. This is the first neptunium complex that has been characterized using single-crystal x-ray diffraction with a synchrotron radiation source. The highly symmetrical structure helps to explain the "silence" of the optical absorption spectra of $NpO_2(L)_2^+$ because the $f \rightarrow f$ transition is completely forbidden. The structure also suggests approaches for rational design of ligands to improve the binding ability with Np(V) and the separation of neptunium from nuclear wastes.

(G. Tian, J. Xu, L. Rao, *Angew. Chem. Int. Ed*. 44, 6200, 2005.)

Presentation plan

1. Why use synchrotron radiation?
2. Single crystal diffraction
    1. Polychromatic
    2. Monochromatic
3. Powder diffraction
    1. Monochromatic
    2. Polychromatic

Monochromatic and Energy-dispersive

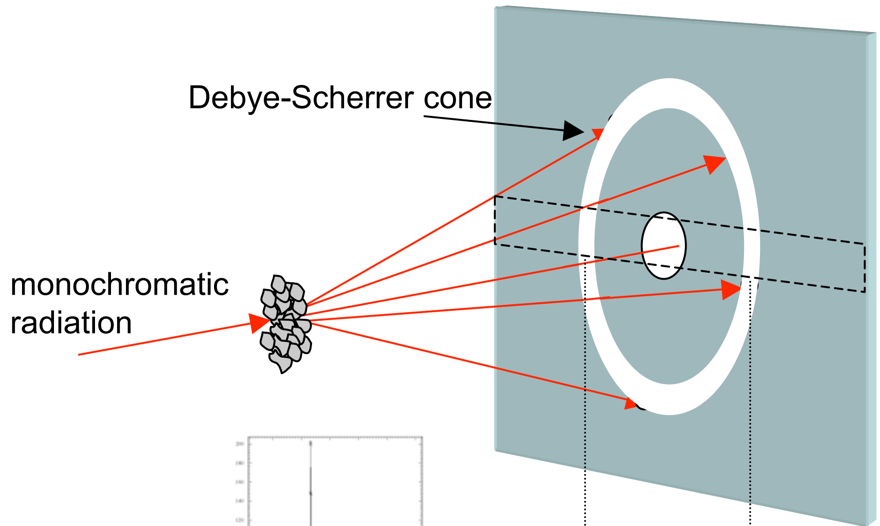

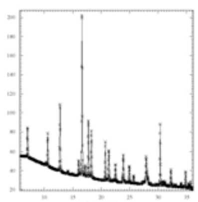

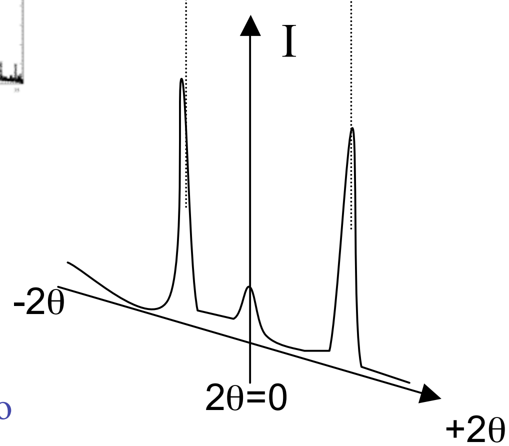

Braggs law

$$\lambda_{hkl} = 2\, d_{hkl} \sin\, \theta$$

λ = wavelength (A)
θ = diffraction angle
d = distance between two planes of atoms

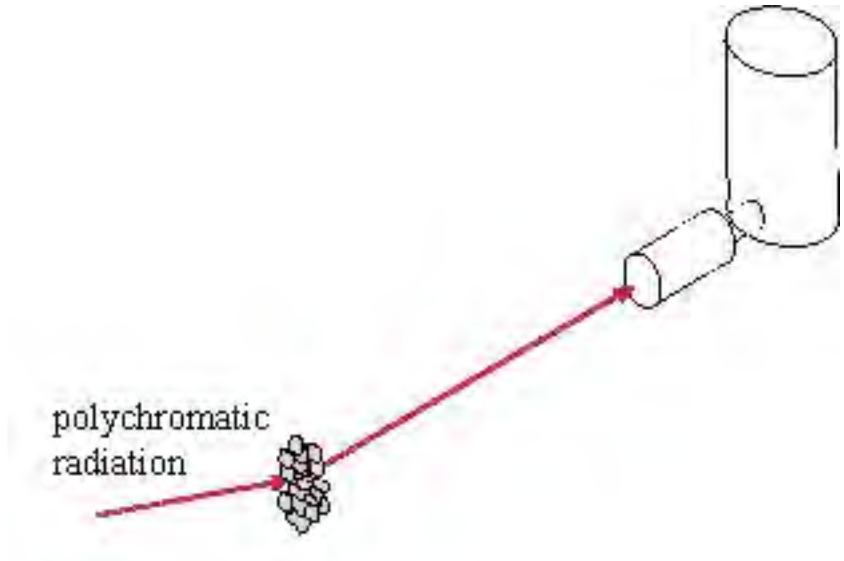

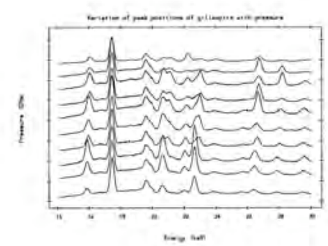

Braggs law

$$E = 6.199 \,/\, d_{hkl} \sin\, \theta$$

E = Energy (keV)
θ = diffraction angle
d = distance between two planes of atoms

Presentation plan

1. Why use synchrotron radiation?
2. Single crystal diffraction
    1. Polychromatic
    2. Monochromatic
3. Powder diffraction
    1. Polychromatic
    2. Monochromatic

In-situ, time-resolved studies of Hydrothermal formation of minerals

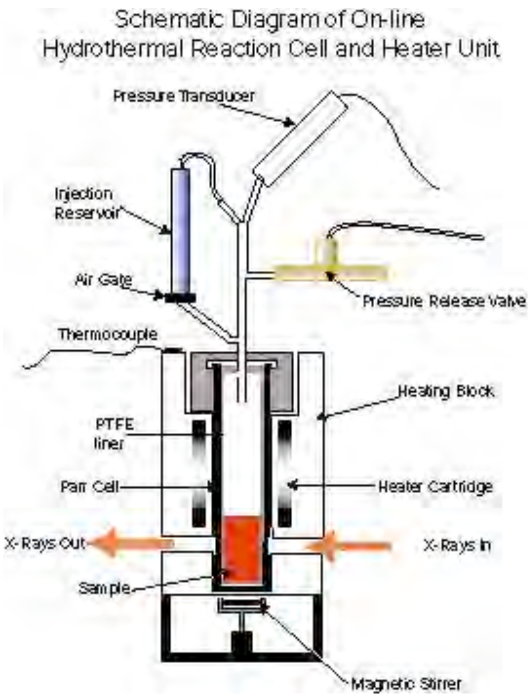

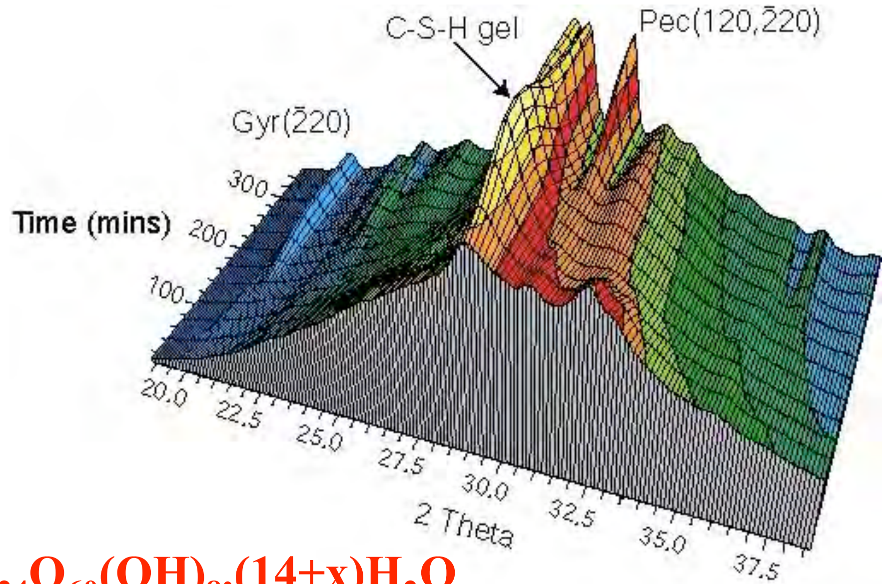

gyrolite $Ca_{16}Si_{24}O_{60}(OH)_8.(14+x)H_2O$
pectolite $Ca_2NaH(SiO_3)_3$

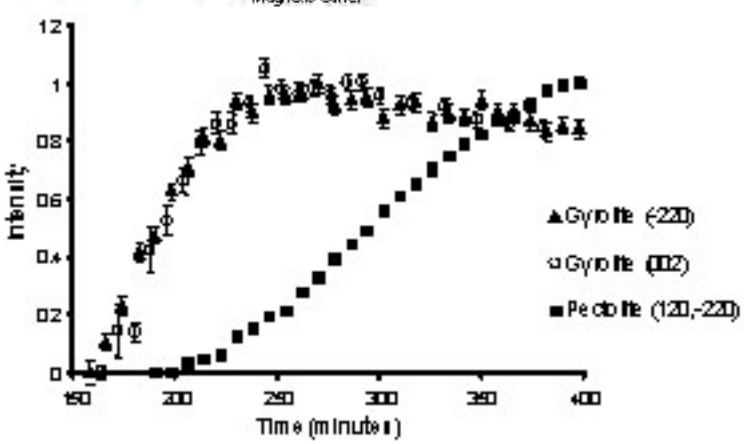

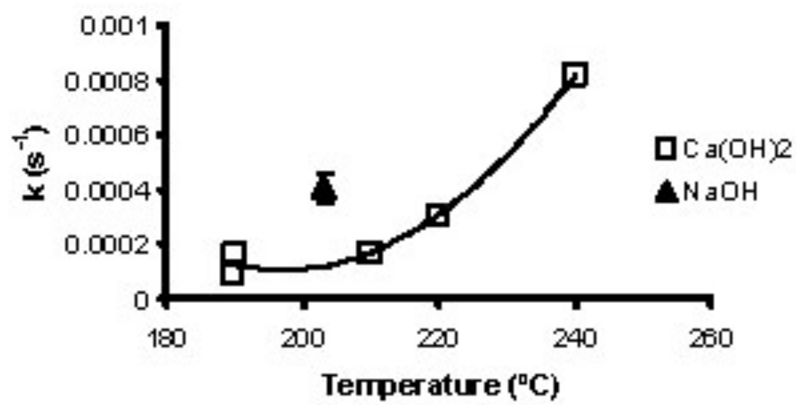

S. Shaw, C.M.B. Henderson and S.M. Clark, *High Pres. Res*. 26(1-6) 311-324 (2001).

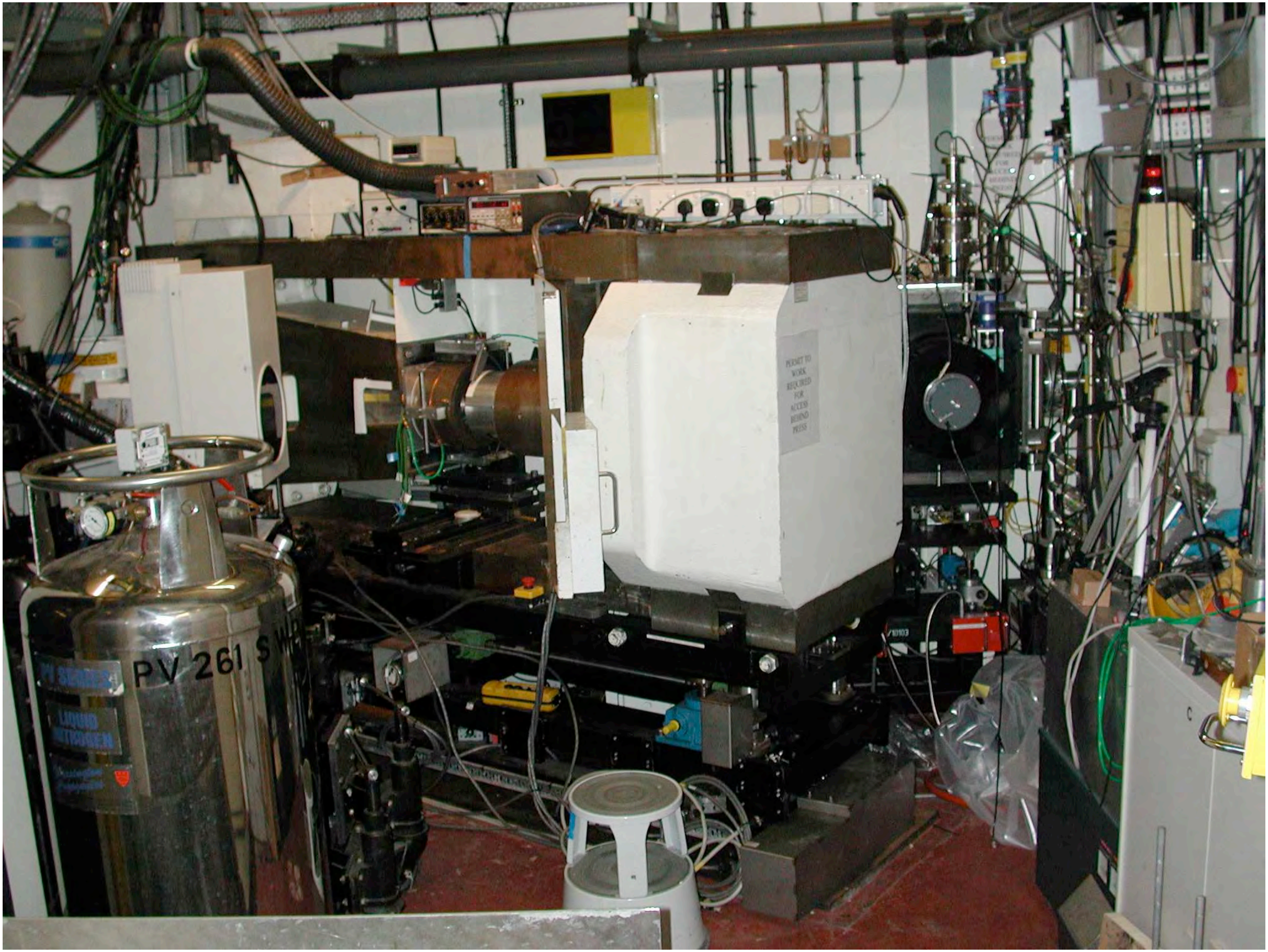
PERMIT TO
WORK
REQUIRED
FOR
ACCESS
BEHIND
PRESS
PV 261 S
PV SERIES
LIQUID
NITROGEN

Walker Cell

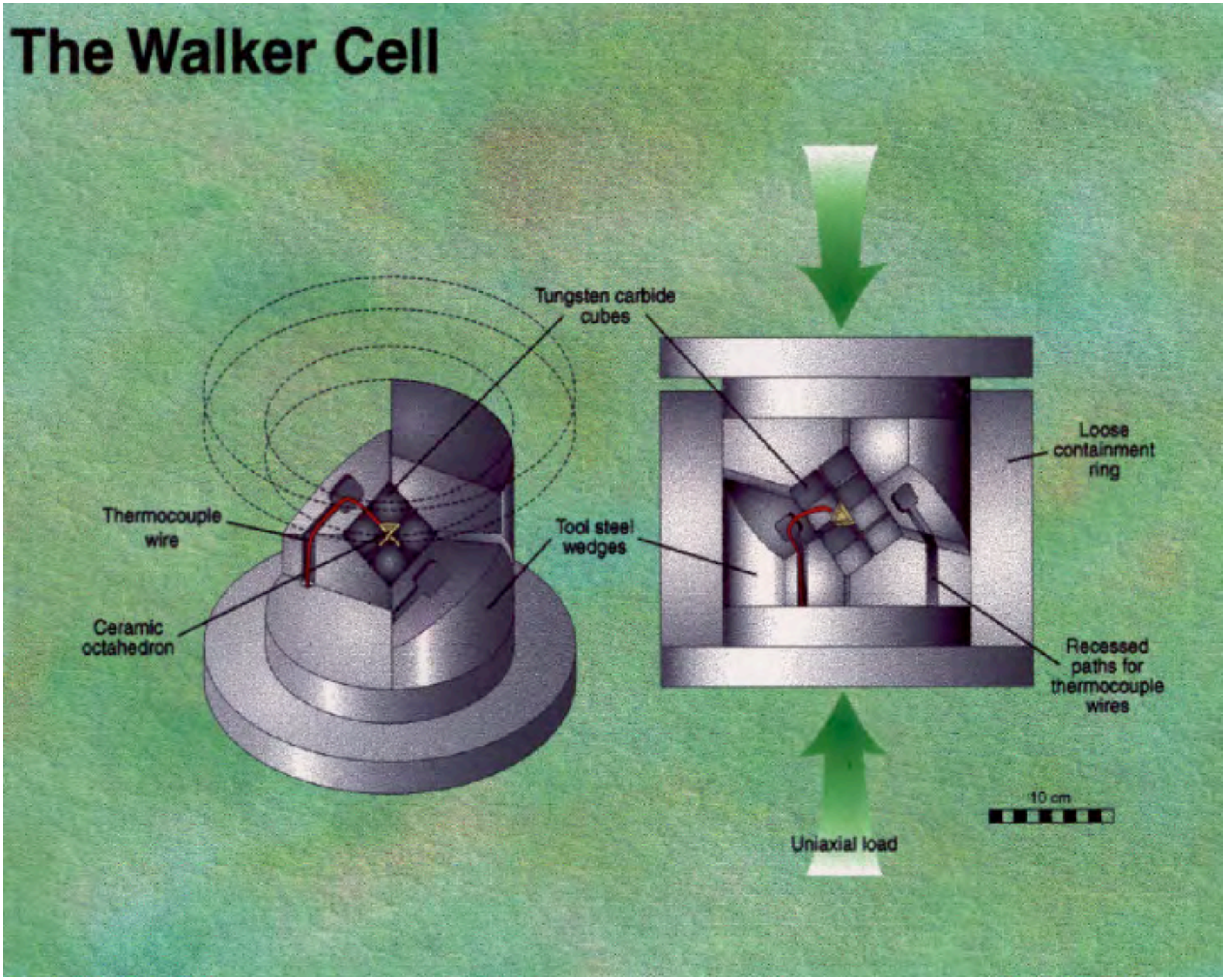

The Walker Cell
Tungsten carbide cubes
Loose containment ring
Thermocouple wire
Tool steel wedges
Ceramic octahedron
Recessed paths for thermocouple wires
10 cm
Uniaxial load

Tungsten carbide cubes

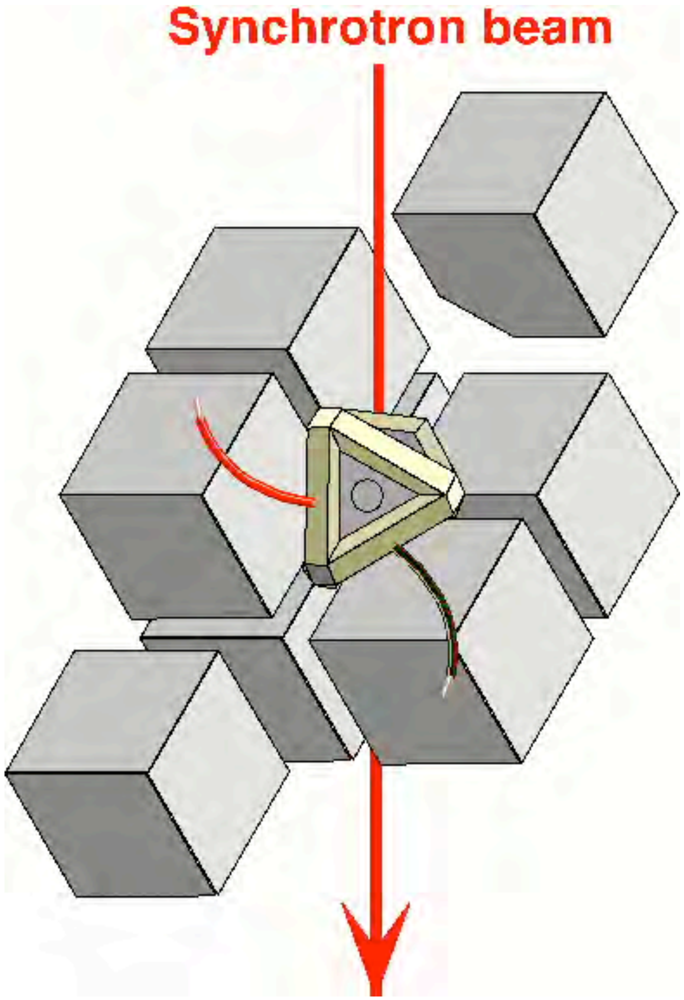

Effect of pressure on the structure of talc

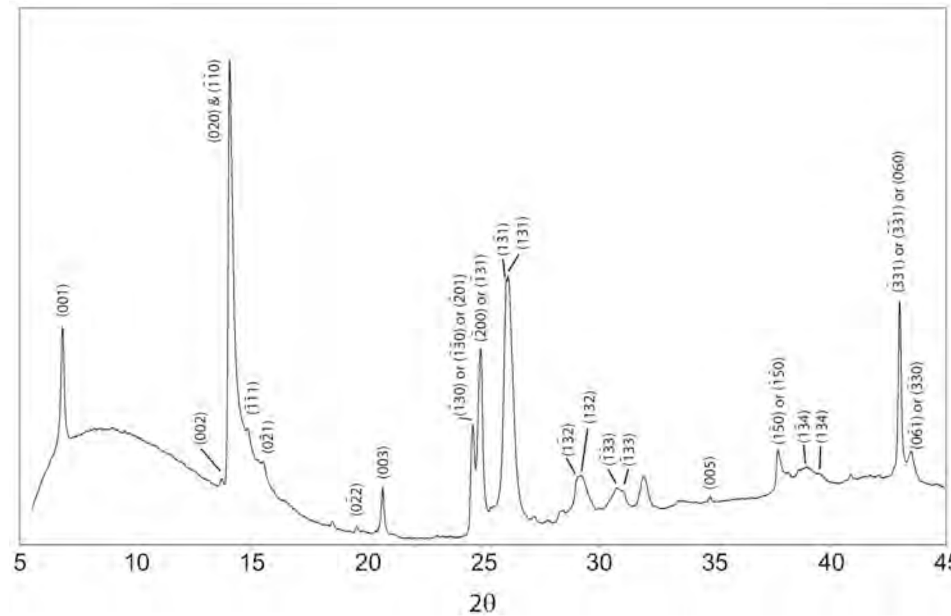

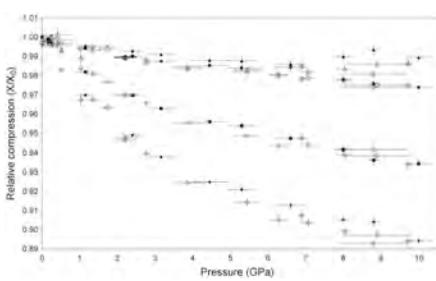

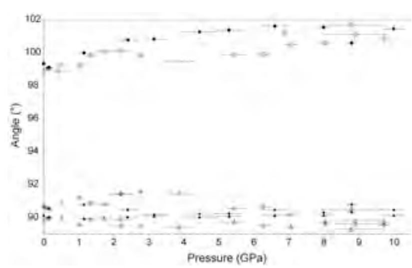

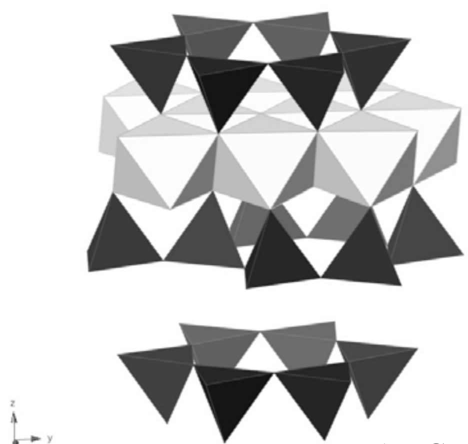

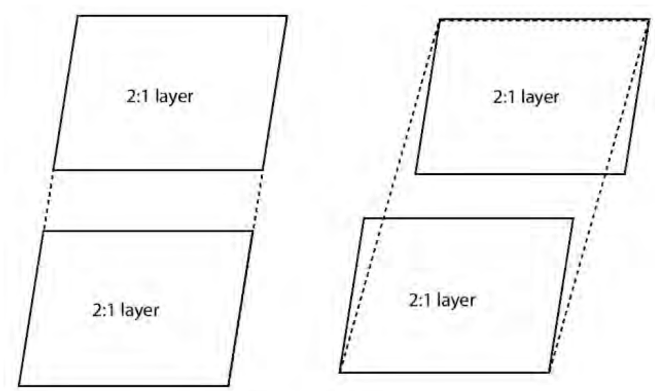

A.E.Gleason, S. Parry, A.R. Pawley and S.M. Clark, *Am. Min*. In Prep. (2005).

Formation of 10A phase ($(Mg_3Si_4O_{10}(OH)_2.xH_2O)$)

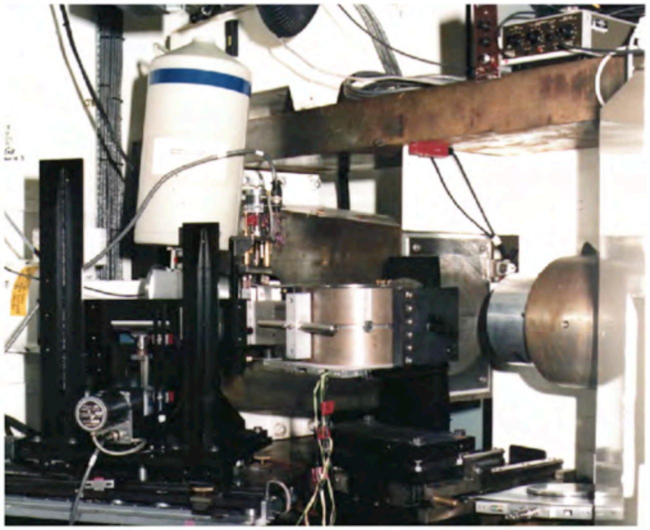

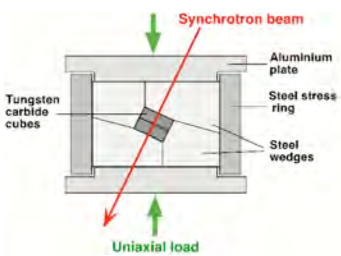

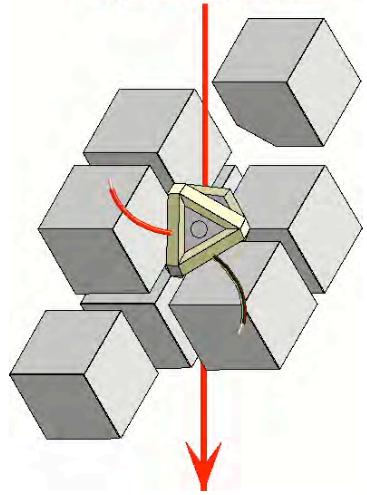

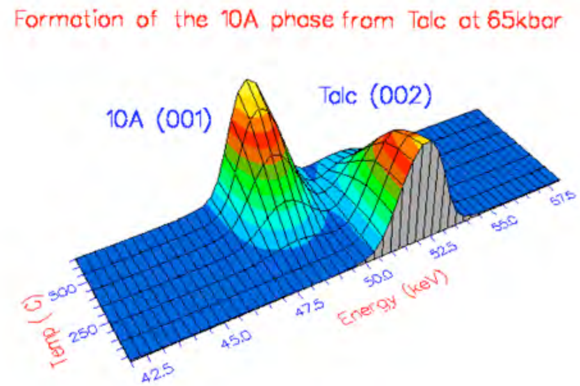

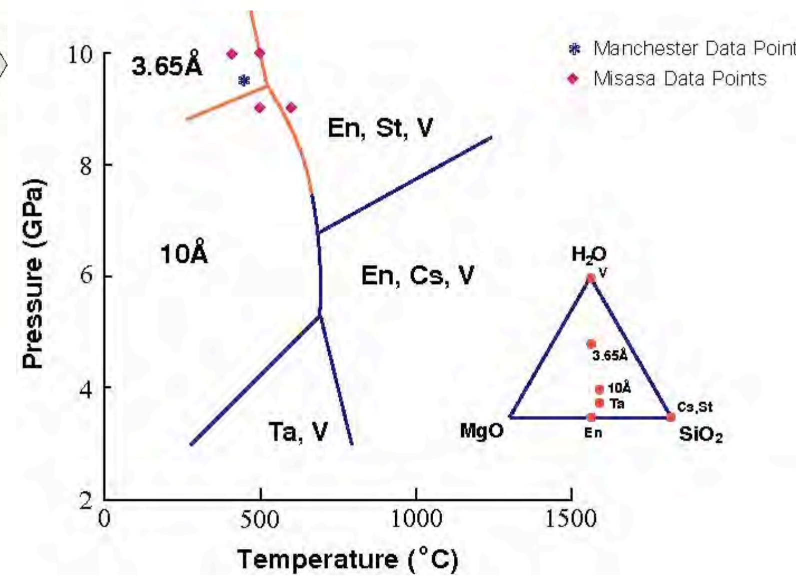

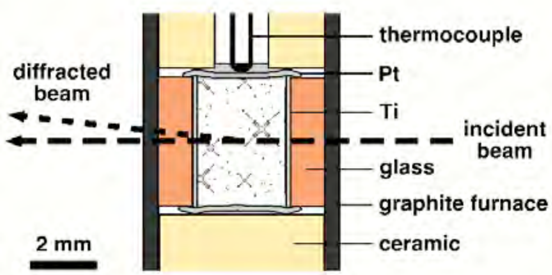

N.J. Chinnery, A.R. Pawley and S.M. Clark, *Science* 286 940-942 (1999).

Presentation plan

1. Why use synchrotron radiation?
2. Single crystal diffraction
    1. Polychromatic
    2. Monochromatic
3. Powder diffraction
    1. Polychromatic
    2. Monochromatic

Diamond Anvil Cell

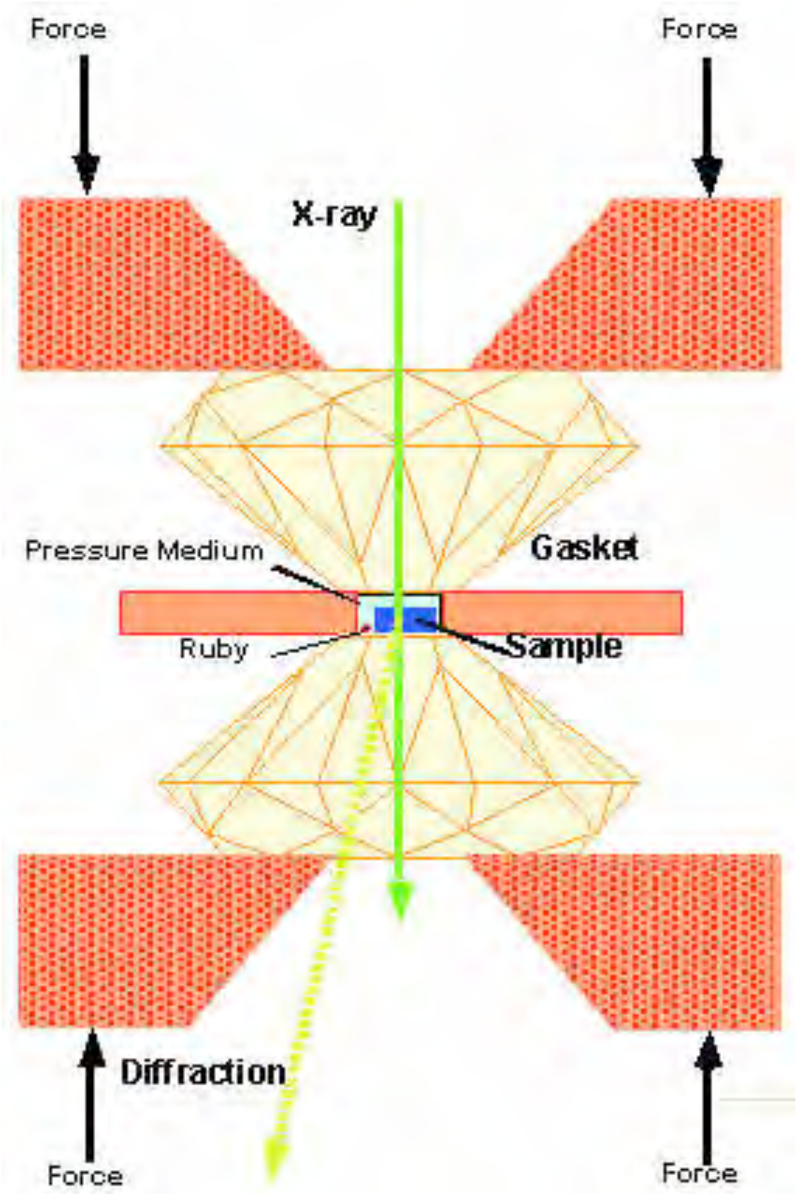

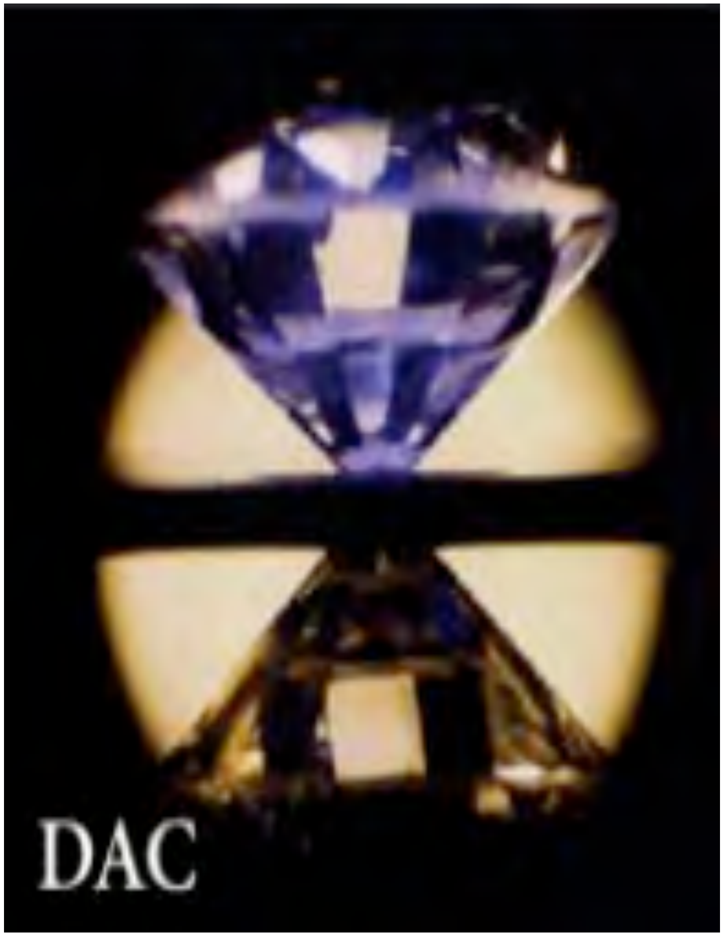

Diamond Anvil cells

Loaded cell

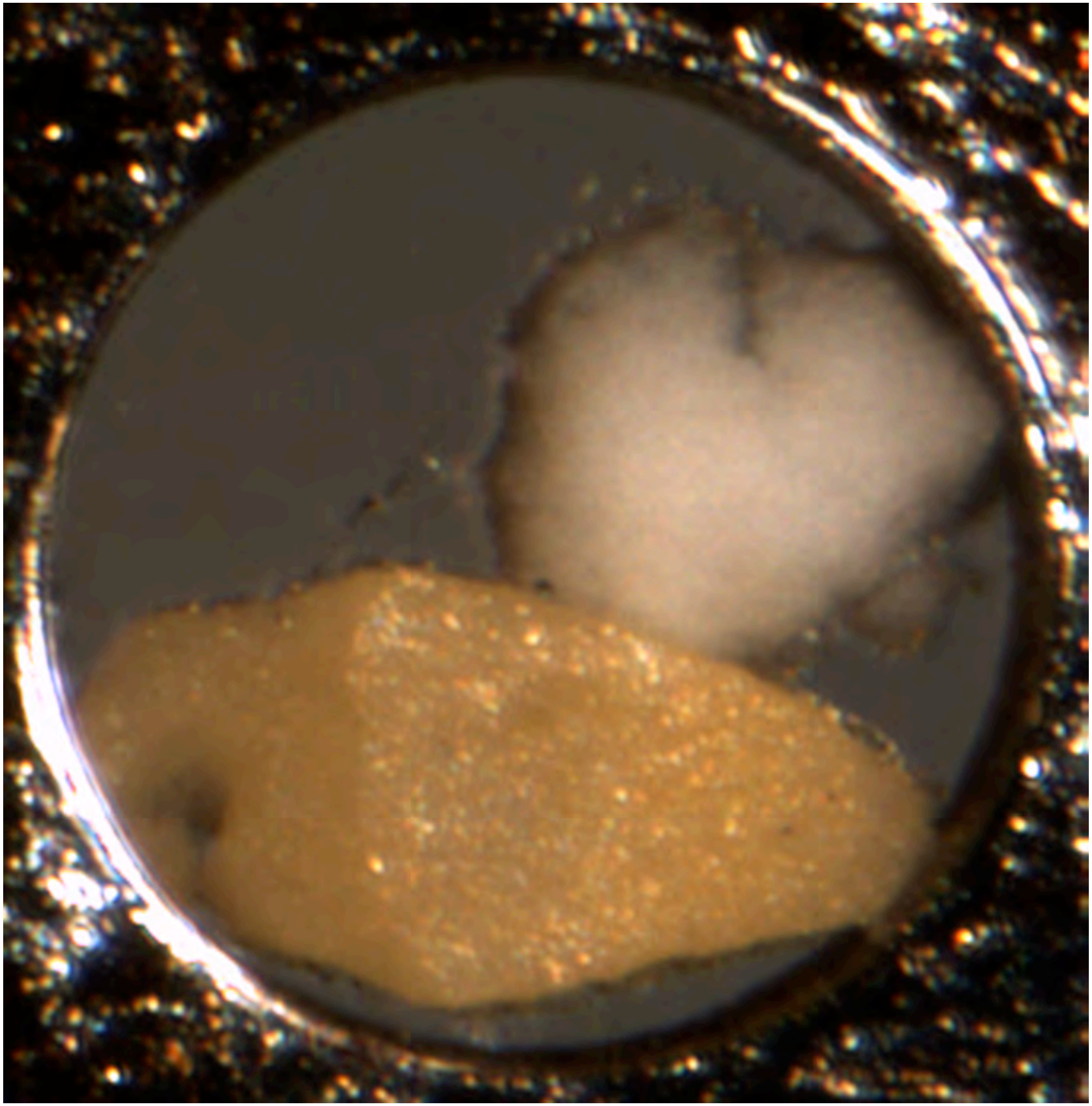

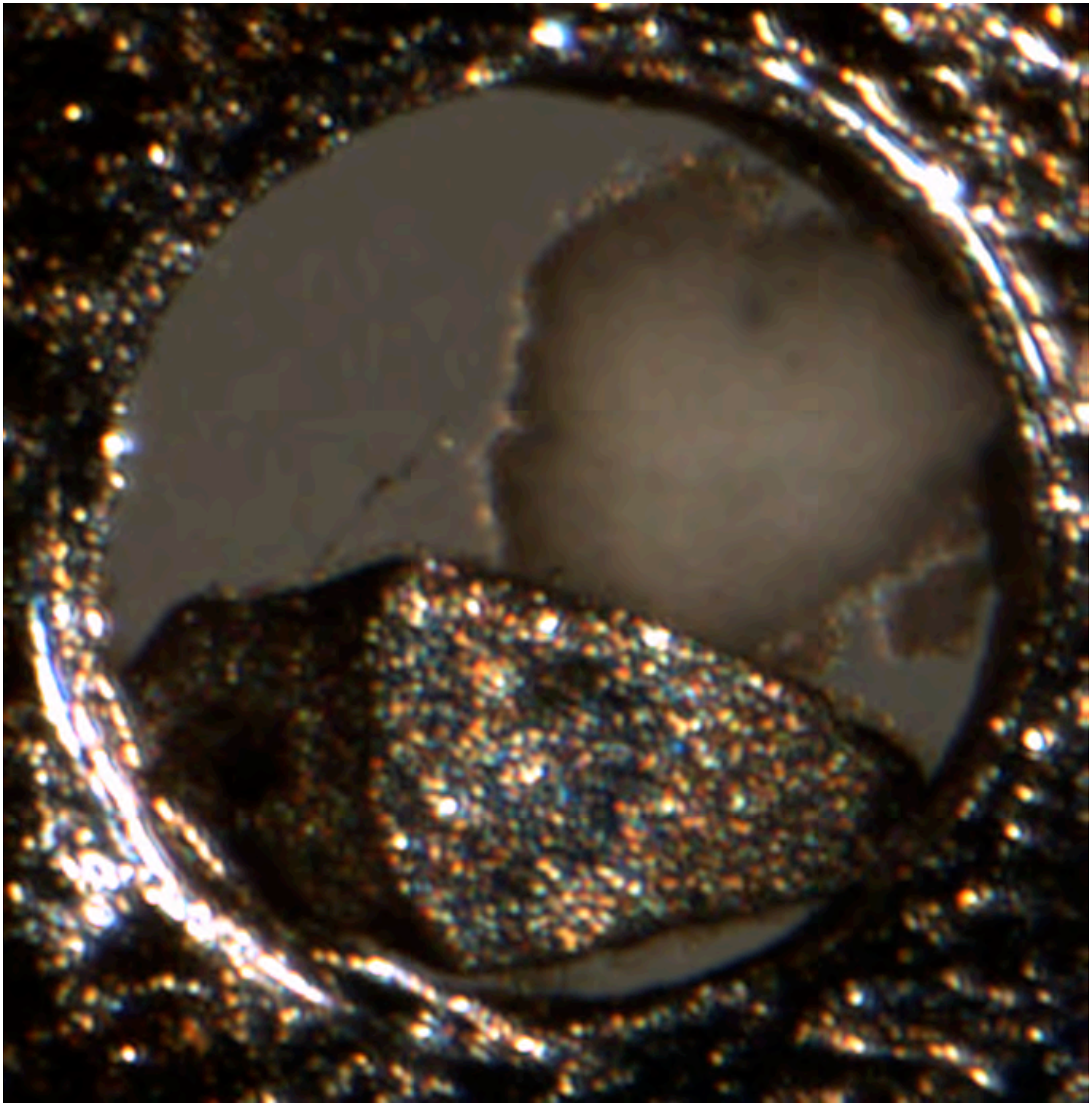

A study of the high-low spin transition in $Mg_{1-x}Fe_xO$

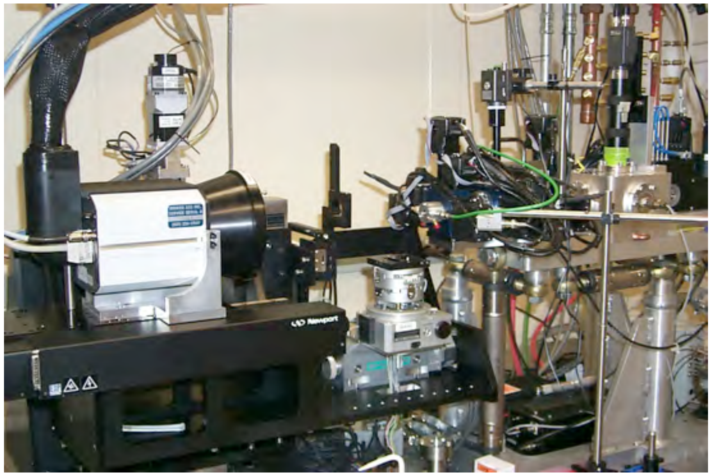

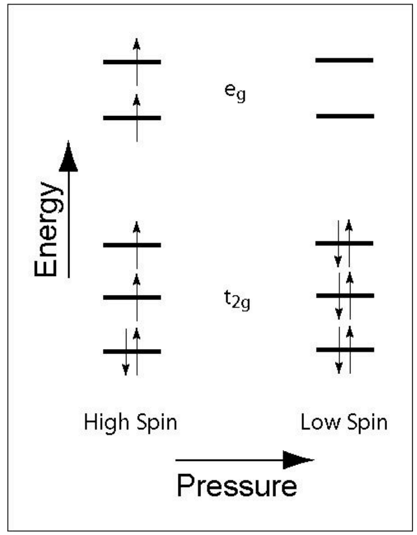

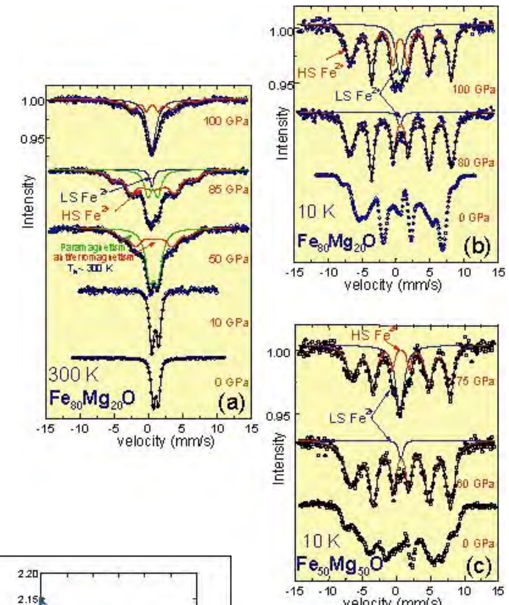

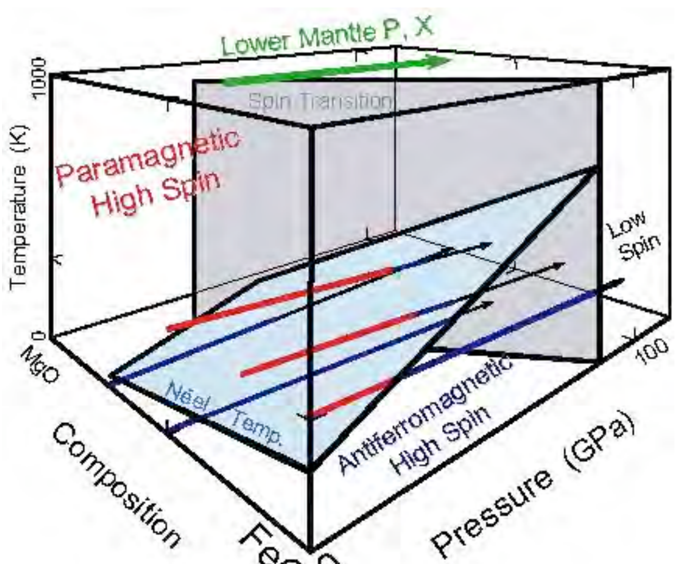

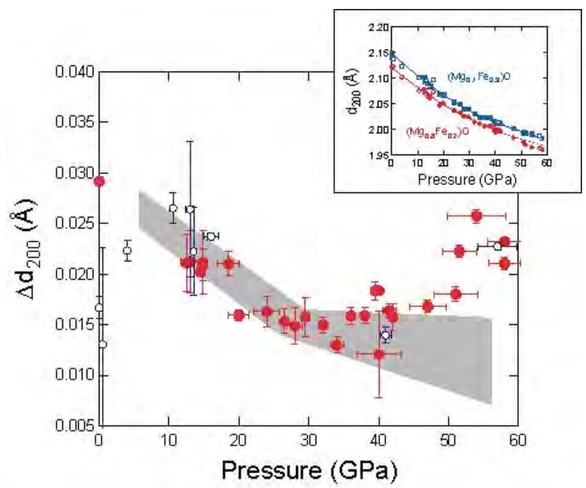

A.A. Milner, S. Speziale, V.E. Lee, S.M. Clark, M.P. Pasternak, and R. Jeanloz, Spin Transition in Earth's Mantle, *PNAS*, 105, 17918-17922 (2005).

Beamline 12.2.2 at the ALS

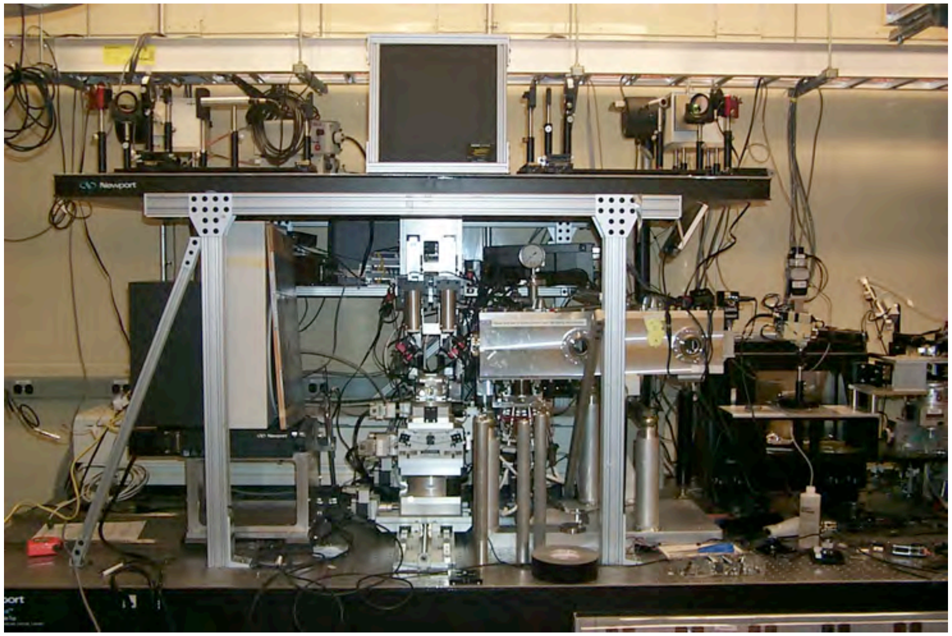

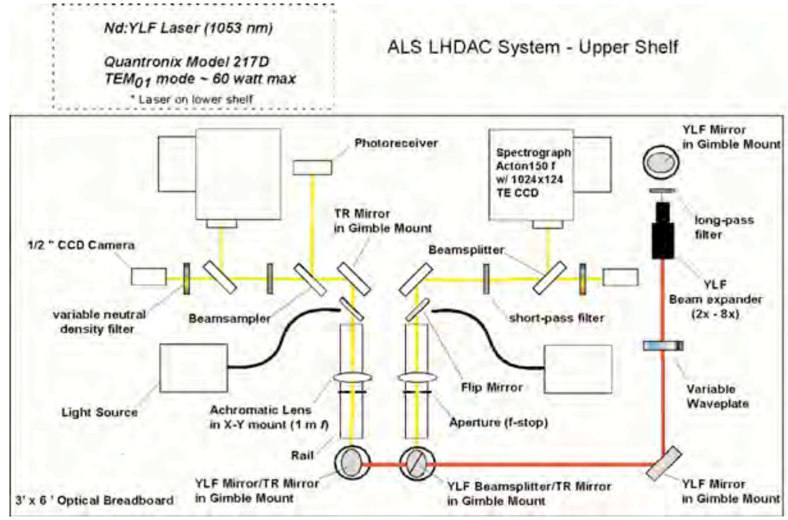

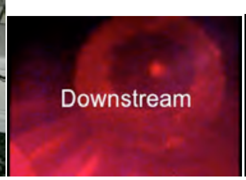

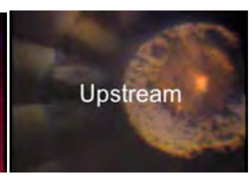

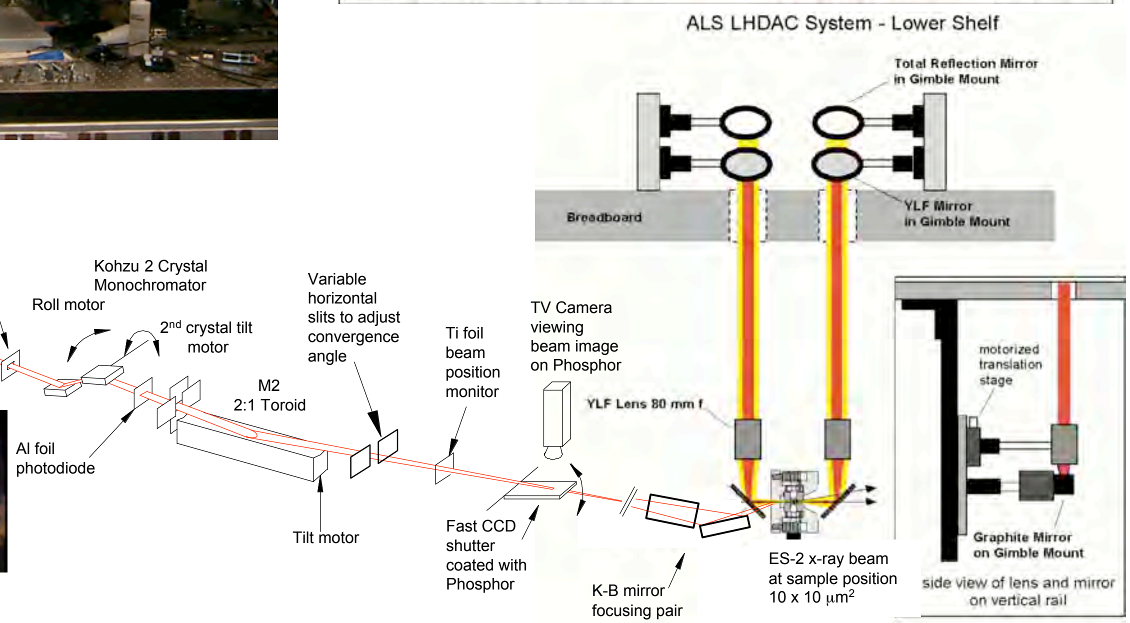

M. Kunz, A.A. MacDowell, W.A. Caldwell, D. Cambie, R.S. Celestre, E.E. Domning, R.M. Duarte, A.E. Gleason, J.M. Glossinger, N. Kelez, D.W. Plate, T. Yu, J.M. Zaug, H.A. Padmore, R. Jeanloz, A.P. Alivisatos, and S.M. Clark. *J. Synch. Rad.* **12(5)** 650-658 (2005).

Review

1. Why use synchrotron radiation?
2. Single crystal diffraction
   1. Polychromatic
   2. Monochromatic
3. Powder diffraction
   1. Polychromatic
   2. Monochromatic